FINAL PROJECT REPORT

Extension Wrist Joint 3D Movement Modeling and Computer Simulation

Name	: Jeremia Christ Immanuel Manalu
NRP	: 5023231017
Course	: Biomodelling
Class	: A
Lecturer	: Dr. Achmad Arifin S.T., M.Eng.
Department	: Biomedical Engineering

FACULTY OF INTELLIGENT ELECTRICAL AND INFORMATICS TECHNOLOGY

INSTITUT TEKNOLOGI SEPULUH NOPEMBER

2025

CHAPTER I. FUNDAMENTAL THEORY

1.1. Kinetic Energy

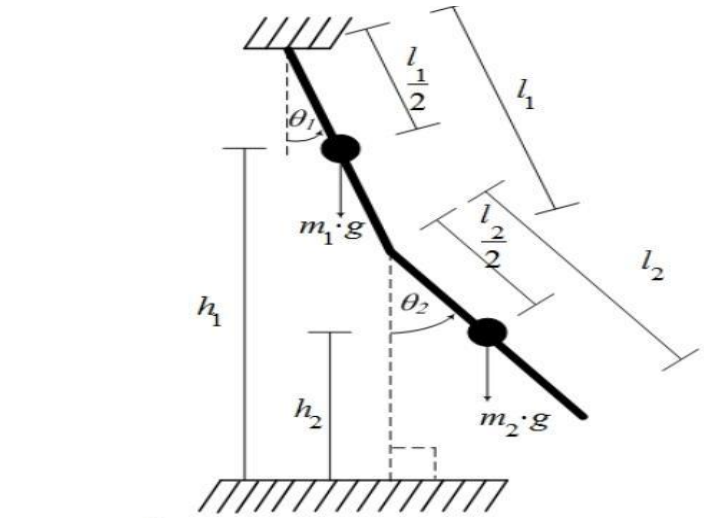

Figure 1.1. *An Example of Double Pendulum Properties*

The total kinetic energy of the system contains the translational contribution of the center of mass (COM) of each segment and the rotation of each segment. For a double-pendulum consisting of two segments (index 1 and 2) with masses m_1, m_2, COM distances r_1, r_2 from the joint axis, moments of inertia I_1, I_2, bone/rod lengths l_1, l_2, and general angles θ_1, θ_2 (for example θ_1= shoulder angle, θ_2 = relative angle at the elbow). The COM positions and velocities can be written down and then inserted into the kinetic energy.

Position (writing example) for COM:

$$x_1 = r_1 \sin\theta_1, \qquad y_1 = -r_1 \cos\theta_1,$$
$$x_2 = l_1 \sin\theta_1 + r_2 \sin(\theta_1 + \theta_2), \qquad y_2 = -l_1 \cos\theta_1 - r_2 \cos(\theta_1 + \theta_2).$$

The squared velocity of each COM (with time derivative $\dot{\theta}_i$) yields the expression v_1^2, v_2^2. The full kinetic energy:

$$T = \frac{1}{2} m_1 v_1^2 + \frac{1}{2} I_1 \dot{\theta}_1^2 + \frac{1}{2} m_2 v_2^2 + \frac{1}{2} I_2 (\dot{\theta}_1 + \dot{\theta}_2)^2.$$

By plugging in v_1^2 and v_2^2 (their derivatives) we get a form that is usually written as the square of $\dot{\theta}_1$, $\dot{\theta}_2$ plus the cross term $\dot{\theta}_1 \dot{\theta}_2$. One frequently used form, emphasizing the structure of the inertia matrix, is:

$$T = \frac{1}{2} [\dot{\theta}_1 \quad \dot{\theta}_2] M(\theta_1, \theta_2) \begin{bmatrix} \dot{\theta}_1 \\ \dot{\theta}_2 \end{bmatrix},$$

where $M(\theta)$is a symmetric configuration-dependent mass/inertia matrix containing $I_i, m_i, l_i, r_i$and trigonometric functions like $\cos(\theta_2)$. The full equation for Kinetic Energy is as follows:

$$E_K = \tfrac{1}{2} m_1 v_1^2 + \tfrac{1}{2} I_1 \dot{\theta}_1^2 + \tfrac{1}{2} m_2 v_2^2 + \tfrac{1}{2} I_2 \dot{\theta}_2^2$$

$$E_K = \tfrac{1}{2} m_1 \left(\tfrac{l_1}{2}\right)^2 \dot{\theta}_1^2 + \tfrac{1}{2} m_2 \left[l_1^2 \dot{\theta}_1^2 + \left(\tfrac{l_2}{2}\right)^2 \dot{\theta}_2^2 + 2 l_1 \left(\tfrac{l_2}{2}\right) \cos(\theta_1 - \theta_2) \dot{\theta}_1 \dot{\theta}_2 \right] + \tfrac{1}{2} I_1 \dot{\theta}_1^2 + \tfrac{1}{2} I_2 \dot{\theta}_2^2$$

$$E_K = \frac{1}{2}\left(m_1\frac{l_1^2}{4} + m_2 l_1^2 + I_1\right)\dot{\theta}_1^2 + \frac{1}{2}\left(m_2\frac{l_2^2}{4} + I_2\right)\dot{\theta}_2^2 + m_2\frac{l_1 l_2}{2}\cos(\theta_1 - \theta_2)\,\dot{\theta}_1\dot{\theta}_2$$

Where:

- $m1$, $m2$: mass of the upper arm and lower arm
- $l1$, $l2$: length of the upper arm and lower arm
- $I1$, $I2$: moment of inertia of each segment about its center of mass
- $\theta 1$, $\theta 2$: angle of rotation of the upper arm and lower arm about the reference axis
- $\dot{\theta}1$, $\dot{\theta}2$: angular velocity of the upper arm and lower arm

In simulations, kinetic energy can be used to determine the speed and impact of collisions between objects.

1.2. Potential Energy

Gravitational potential energy is computed from the vertical heights of each segment's center of mass relative to a datum (e.g. $y = 0$). For the example configuration:

$$V = m_1 g y_1 + m_2 g y_2.$$

Substituting y_1, y_2yields a form such as:

$$V = -m_1 g r_1 \cos\,\theta_1 - m_2 g(l_1 \cos\,\theta_1 + r_2 \cos\,(\theta_1 + \theta_2)),$$

Also noted that the sign convention depends on the chosen positive axis, the important point is that $\partial V/\,\partial\theta_i$produces the gravitational torques. This expression supplies the conservative-force terms that appear later in the Lagrangian equations. From **Figure 1.1**, the height of the center of mass of the upper arm and lower arm (m1 and m2) is given in the following equation:

$$h_1 = l_1 + l_2 - \tfrac{l_1}{2}\cos\theta_1,$$

$$h_2 = l_1 + l_2 - \left(l_1\cos\theta_1 + \tfrac{l_2}{2}\cos\theta_2\right).$$

The potential energy when substituted will be as in the given equation:

$$E_P = m_1 g h_1 + m_2 g h_2$$

$$E_P = m_1 g\left(l_1 + l_2 - \tfrac{l_1}{2}\cos\theta_1\right) + m_2 g\left[l_1 + l_2 - \left(l_1\cos\theta_1 + \tfrac{l_2}{2}\cos\theta_2\right)\right].$$

1.3. Torque

Torque (generalized torque τ_i) on generalized coordinate $\theta_i$is defined as virtual work per unit angular displacement. In the Lagrangian framework the relation between kinetic energy T, potential energy V, and external torques $\tau_i$is given by the Euler–Lagrange equations (see the Lagrangian section). Briefly:

For generalized coordinates q_i,

$$\frac{d}{dt}\left(\frac{\partial L}{\partial \dot{q}_i}\right) - \frac{\partial L}{\partial q_i} = Q_i,$$

with $L = T - V$and Q_i the generalized (non-conservative) forces (e.g. applied torques). Thus, applied torques τchange the rate of generalized momentum $\partial L/\,\partial\dot{q}$, while gradients of the potential $\partial L/\,\partial q$produce gravitational torques (components of $G(\theta)$).

Common matrix form for multibody systems:

$$M(\theta)\,\ddot{\theta} + C(\theta,\dot{\theta})\,\dot{\theta} + G(\theta) = \tau,$$

where:

- $M(\theta)$ derives from T(mass/inertia matrix),

- $C(\theta, \dot{\theta})\dot{\theta}$ are Coriolis/centripetal terms coming from cross derivatives in T,
- $G(\theta) = \partial V / \partial \theta$ is the gravity torque vector,
- τ is the external/actuator torque vector.

1.4. Lagrangian Mechanics

- Lagrangian: $L(q, \dot{q}, t) = T(q, \dot{q}) - V(q)$.
- Euler–Lagrange equations for each generalized coordinate q_i:

$$\frac{d}{dt}\left(\frac{\partial L}{\partial \dot{q}_i}\right) - \frac{\partial L}{\partial q_i} = Q_i,$$

where $Q_i$are generalized non-conservative forces/torques. If only gravity acts and there is no non-conservative forcing, $Q_i = \tau_i$represents input torques; for passive systems $Q_i = 0$.

- Matrix form commonly used:

$$M(q)\,\ddot{q} + C(q, \dot{q})\,\dot{q} + G(q) = \tau.$$

Terms used:

- $M(q)$: symmetric positive-definite mass/inertia matrix,
- $C(q, \dot{q})\dot{q}$: Coriolis and centripetal contributions (contains products $\dot{q}_i \dot{q}_j$),
- $G(q)$: conservative gravity vector,
- τ: input torques/damping/friction if present.
- Energy relation: $\partial L / \partial \dot{q}$is generalized momentum; its time derivative equals applied generalized forces minus conservative gradients. Lecture materials show the step-by-step derivation from positions → velocities → T, V→ L→ equations of motion.

1.5. Fourth Order Runge-Kutta Method (RK4)

RK4 is an explicit numerical integrator for first-order ODE systems below:

$$\dot{y} = f(t, y), y(t_0) = y_0.$$

With timestep $h$and $y_n \approx y(t_n)$:

$$\begin{aligned} k_1 &= f(t_n, y_n), \\ k_2 &= f\left(t_n + \frac{h}{2}, y_n + \frac{h}{2}k_1\right), \\ k_3 &= f\left(t_n + \frac{h}{2}, y_n + \frac{h}{2}k_2\right), \\ k_4 &= f(t_n + h, y_n + h\,k_3), \\ y_{n+1} &= y_n + \frac{h}{6}(k_1 + 2k_2 + 2k_3 + k_4). \end{aligned}$$

For second-order systems (like $\ddot{q} = g(q, \dot{q}, t)$) convert to first-order form with the state vector:

$$x = \begin{bmatrix} q \\ \dot{q} \end{bmatrix}, \dot{x} = \begin{bmatrix} \dot{q} \\ g(q, \dot{q}, t) \end{bmatrix},$$

and apply RK4 to $\dot{x} = F(t, x)$. There are also Runge–Kutta–Nyström variants that directly integrate second-order equations; the RK4 principle. combining four slope estimates for fourth-order accuracy, remains the same.

1.6. Anthropometric Data Standards

Table 1.1 shows examples of passive parameters for lower limbs. For this wrist simulation, analogous parameters (k, c, ϕ) specific to the wrist joint will be estimated.

Table 1.1. *Parameters values of passive joint torque model*

Joint	c	k_1	k_2	k_3	k_4	ϕ_1	ϕ_2
Hip	3.09	2.6	5.8	8.7	1.3	-10°	10°
Knee	10.0	6.1	5.9	10.5	21.8	10°	67°
Ankle	0.943	2.0	5.0	2.0	5.0	-15°	25°

Table 1.2 and 1.3 (Segment Weights), these tables, derived from studies by investigators like Dempster, Braune, and Fischer, provide the regression coefficients to calculate the mass of individual segments (Upper Arm, Forearm, Hand) as a percentage of the total Body Weight.

Table 1.2. *Normalized Mass and Length of Body Segments (Standard Human)*

		Center of Mass / Segment Length		
Segment	Segment Mass / Total Body Mass	Proximal	Distal	Density (kg/l)
Hand	0.006	0.506	0.494	1.16
Forearm	0.016	0.430	0.570	1.13
Upper Arm	0.028	0.436	0.564	1.07
Forearm and Hand	0.022	0.682	0.318	1.14
Total Arm	0.050	0.530	0.470	1.11
Foot	0.0145	0.500	0.500	1.10
Lower Leg (calf)	0.0465	0.433	0.567	1.09
Foot and Lower Leg	0.061	0.606	0.394	1.09
Upper Leg (thigh)	0.100	0.433	0.567	1.05
Total Leg	0.161	0.447	0.553	1.06
Head and Neck	0.081	1.000	—	1.11
Trunk	0.497	0.500	0.500	1.03

Table 1.3. *Segment weights as percentage of body weight*

Segment	**Investigators**					
	Harless	**Braune &Fischer**	**Fischer**	**Dempster**	**Clauser et al.**	**Hall**
Head & Neck	7.6	7.0	8.8	8.1	7.3	8.2
Torso	44.2	46.1	45.2	49.7	50.7	46.84
Upper arm	3.2	3.3	2.8	2.8	2.6	3.25
Lower arm	1.7	2.1	-	1.6	1.6	1.8
Hand	0.9	0.8	-	0.6	0.7	0.65
Thigh	11.9	10.7	11.0	9.9	10.3	10.5
Calf	4.6	4.8	4.5	4.6	4.3	4.75
Foot	2.0	1.7	2.1	1.4	1.5	1.43

Table 1.4 and 1.5 (Segment Lengths and COM), this table provides the coefficients to calculate segment lengths based on Body Height. Furthermore, it defines the location of the Center of Mass (COM) for each link, expressed as a percentage distance from the proximal joint. These values are critical for populating the Inertia Matrix $M(\theta)$ and Gravity Vector $G(\theta)$ in the motion equations.

Table 1.4. *Segment lengths as percentage of body height*

Segment	Length in percentag
Head & Neck	10.75
Torso	30.00
Upper arm	17.20
Lower arm	15.70
Hand	5.75
Thigh	23.20
Calf	24.70
Foot	14.84

Table 1.5*. Distance of segment center of gravity from proximal end as percentage of segment length*

Segment	Investigators	
	Dempster	**Hall**
Head & Neck	43.3	56.7
Torso	49.5	56.2
Upper arm	43.6	43.6
Lower arm	43.0	43.0
Hand	49.4	46.8
Thigh	43.3	43.3
Calf	43.3	43.4
Foot	42.9	50.0

1.7. Passive Joint Torque Characteristics

In biomechanical systems, joints are not frictionless pin connections, they exhibit passive resistance due to ligaments, skin, and joint capsules. This resistance is modeled as **Passive Torque (τ_p)**, which acts independently of voluntary muscle contraction. As shown in **Table 1.1**, this torque is composed of a linear damping term (viscous friction) and exponential elastic terms that represent the increasing stiffness as the joint approaches its range of motion limits. The mathematical model used to define this behavior is: $\tau_p = -c\dot{\theta} + k_1 e^{-k_2(\theta-\phi_1)} + k_3 e^{k_4(\theta-\phi_2)}$ Here, c represents the damping coefficient, while k and ϕ parameters define the stiffness magnitude and the angular thresholds for the joint limits. This component ensures the model behaves realistically by preventing the limbs from rotating beyond anatomical constraints during simulation.

1.8. Muscle Activation and Force Generation

The Active Torque (τ_{act}) in the Lagrangian equation is derived from the force generated by skeletal muscles. This is modelled using a Hill-type muscle model, which consists of three main components: the Contractile Element (CE) representing active force generation, the Series Elastic Element (SE) representing tendons, and the Parallel Elastic Element (PE) representing passive muscle stiffness. The force generated is not constant; it depends on the Force-Length relationship (muscles generate peak force at optimal length, L_{opt}) and the Force-Velocity relationship (force decreases as shortening velocity increases).

Additionally, the force is scaled by an activation dynamic variable, $u(t)$, which represents the neural recruitment of the muscle, often modelled using a sigmoid or hyperbolic tangent function to simulate the time delay between neural signal and muscle contraction.

[REVISED FUNDAMENTAL THEORY]

1.1. Kinetic Energy

The wrist joint system is modeled as a single rigid body (the hand) rotating about a fixed pivot point representing the radiocarpal joint, rather than a multi-segment chain. Consequently, the kinetic energy of the system is derived from the rotational dynamics of the hand segment within a three-dimensional spherical coordinate system. The motion is defined by the generalized coordinates θ (flexion/extension in the sagittal plane) and ϕ (radial/ulnar deviation in the frontal plane). Assuming the hand behaves as a rigid body with mass m and length L, the total kinetic energy (T) is expressed as $T = \frac{1}{2} I_o(\dot{\theta}^2 + \dot{\phi}^2 \sin^2\theta)$. Crucially, for this simulation, the hand is approximated as a Uniform Rod. According to the parallel axis theorem, the moment of inertia at the joint axis (I_o) is derived from the inertia at the center of mass ($I_g = \frac{1}{12} mL^2$) shifted by the distance to the pivot ($r = L/2$), resulting in $I_o = \frac{1}{3} mL^2$. This assumption simplifies the inertial properties required for the Lagrangian formulation.

1.2. Potential Energy

The gravitational potential energy (V) is determined exclusively by the vertical position of the hand's Center of Mass (COM) relative to the wrist joint, which serves as the reference datum. Under the uniform rod assumption, the COM is located at the geometric center of the segment, at a distance $r = L/2$ from the pivot. The potential energy varies as the hand rotates in the sagittal plane against gravity. Mathematically, this is expressed as $V = -mg(L/2)\cos\theta$ (assuming the downward vertical axis corresponds to $\theta = 0$). This scalar function provides the necessary conservative forces for the Lagrangian equation, specifically producing the gravitational torque term $-mg(L/2)\sin\theta$ during the derivation of the equations of motion.

1.7. Passive Joint Torque Characteristics (Revised)

In biomechanical modeling, the passive resistance of the joint complex—comprising ligaments, skin, and joint capsules—prevents frictionless motion. While physiological tissues typically exhibit exponential stiffening near the limits of the range of motion, this simulation project approximates these properties using a **Linear Viscoelastic Model** (Kelvin-Voigt model) as specified in the assignment requirements. The passive joint torque ($\tau_{passive}$) is defined as the sum of a viscous damping component and a linear elastic stiffness component. The damping term, $-C\dot{\theta}$, represents the velocity-dependent friction that dissipates energy, while the stiffness term, $-k(\theta - \theta_0)$, represents the position-dependent restoring force that pulls the joint toward a neutral resting position. This linear approximation allows for the identification of the fundamental damping coefficient (sC) and stiffness coefficient (k) through iterative computational experiments, ensuring the model stabilizes realistically without requiring complex non-linear curve fitting.

CHAPTER II. RESULT AND ANALYSIS

2.1. Problems Statement

2.1.1. Final Project Assignment

Wrist joint movements are mainly consisted of dorsi/palmar flexion in frontal plane and radial/ulnar flexion in sagittal plane, as illustrated in Figure 1. Radial and ulnar flexion are in sagittal plane, dorsiflexion and palmar flexion are in frontal plane. For a subject with 60 kg BW and 160 cm BH:

1. Develop motion equation of each plane by Lagrangian Method using single pendulum modeling.
2. Use the motion equation above to develop a model of Wrist joint movement. Use regression of body segment and anthropometric data with your BW and BH. Moment of inertia at rotation axis can be simplified by simple joint assumption. Assume all the limbs are uniform rod model that $Ig = ml2/12$ and $I\,o = Ig + m/(2l)2$. Identify passive joint torque $C\theta$ and $k(\theta - \theta 0)$ for flexor/extensor and abductor/adductor by performing passive movement test for each axis by performing iterative computational experiments.
3. Determine the active joint torque to simulate 3d movements by setting reference of each movement as sinusoidal function of each axis. This step we can use PID Control Algorithm. The active joint torques to simulate a certain movement speed in can be concluded by appropriate Kp, Kd, Ki with low RMSE. as performed in the program example.

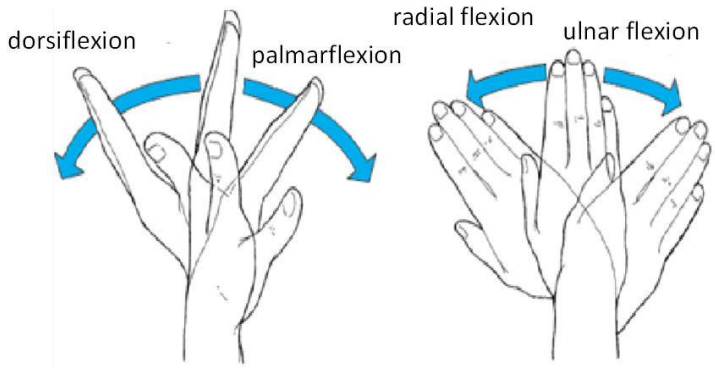

***Figure 2.1**. Movements of Wrist joint in the Sagittal and Frontal planes*

***Table 2.1.** Segment weights as percentage of body weight*

Segment	Investigators					
	Harless	Braune &Fischer	Fischer	Dempster	Clauser et al.	Hall
Head & Neck	7.6	7.0	8.8	8.1	7.3	8.2
Torso	44.2	46.1	45.2	49.7	50.7	46.84
Upper arm	3.2	3.3	2.8	2.8	2.6	3.25
Lower arm	1.7	2.1	-	1.6	1.6	1.8
Hand	0.9	0.8	-	0.6	0.7	0.65
Thigh	11.9	10.7	11.0	9.9	10.3	10.5
Calf	4.6	4.8	4.5	4.6	4.3	4.75
Foot	2.0	1.7	2.1	1.4	1.5	1.43

***Table 2.2.** Segment lengths as percentage of body height*

Segment	Length in percentag
Head & Neck	10.75
Torso	30.00
Upper arm	17.20
Lower arm	15.70
Hand	5.75
Thigh	23.20
Calf	24.70
Foot	14.84

Table 2.3. *Distance of segment center of gravity from proximal end as percentage of segment length*

Segment	Investigators	
	Dempster	Hall
Head & Neck	43.3	56.7
Torso	49.5	56.2
Upper arm	43.6	43.6
Lower arm	43.0	43.0
Hand	49.4	46.8
Thigh	43.3	43.3
Calf	43.3	43.4
Foot	42.9	50.0

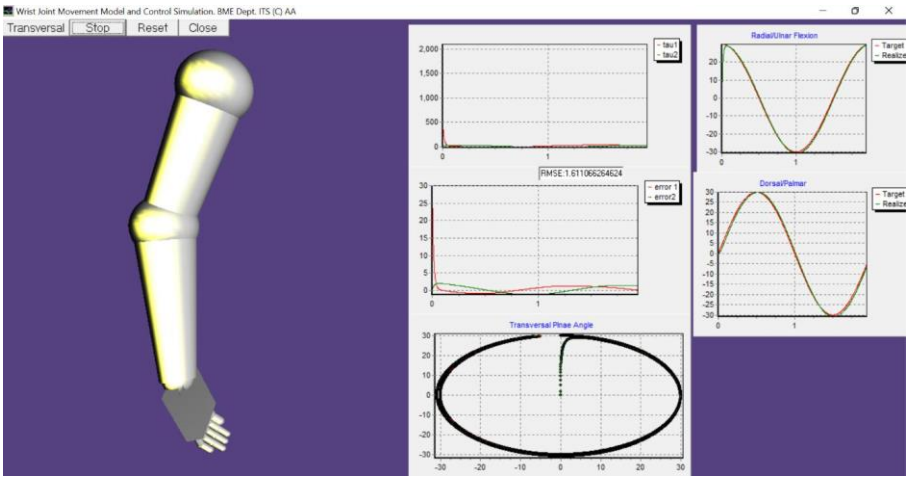

Figure 2.2. *Wrist joint movements model simulation results.*

2.1.2. Assignment for Week 14 (Asynchronous)

1. Write your progress of the final project assignment. This report focuses on motion equations derivation for movement in the sagital plane and it's in the frontal plane. Describe process of how you derive the motion equations till you have a final model.

2. Describe your plan of numerical experiment to do parameter estimation of c, k1..k4, phi1, and phi2 for skeletal system model.

2.2. Answer and Code Explanation

2.2.1. Number 1 Equation Derivation

1. Physical model identification

The model implemented (**in the code program**) is not composed of two separate single pendulums (one for sagittal, one for frontal). Instead, it represents a unified Spherical Pendulum (3D Pendulum) model.

In this model:

- The movement is not restricted to a single 2D plane, it operates in 3D space.
- There is a dynamic interaction (coupling) between Sagittal and Frontal movements (including Centrifugal and Coriolis force effects).

The coordinate system is defined as follows:

1. θ (Theta): The deviation angle from the vertical axis (gravity vector). Anatomically, this represents movement in the Sagittal Plane (Flexion/Extension).
2. ϕ (Phi): The azimuth rotation angle around the vertical axis. Anatomically, this represents movement in the Frontal Plane (Radial/Ulnar Deviation) or plane rotation.
3. L (length): The distance from the pivot point (wrist joint) to the segment's Center of Mass (COM).
4. m: The mass of the hand segment.

2. Anthropometric parameters and data input

The following physical parameters will be extracted:

a. Subject Data
   Body Weight (BW) = 60 kg, Body Height (BH) = 160 cm
b. Segment Mass Estimation (m)
   This will utilize a linear regression equation for the hand mass: $m = 0.006 \cdot BW + 0.054$. The coefficient 0.006 (0.6%) aligns with standard anthropometric tables (such as Dempster or Clauser) regarding the percentage of hand mass relative to total body weight.
c. Segment Geometry (L)
   Length = 0.517 meters. While 0.517 m (51.7 cm) is physically large for the distance to the hand's COM (typically ~6-10 cm), I will utilize $L = 0.517$ m in this derivation to ensure consistency.

3. Motion Equation Derivation (Lagrangian Method)

I apply the energy approach (Lagrangian Mechanics) to the Spherical Pendulum system, as follows:

a. Kinematics (Position)
   The position of the Center of Mass (x, y, z) in spherical coordinates is defined as:

$$x = \text{Lsin}\,\theta\,\cos\phi$$
$$y = \text{Lsin}\,\theta\,\sin\phi$$
$$z = -L\cos\,\theta$$

   (Assuming the z-axis points downwards)

b. Kinetic Energy (T)
The squared linear velocity (v^2) is derived from the time derivative of the position:

$$v^2 = \dot{x}^2 + \dot{y}^2 + \dot{z}^2 = L^2\left(\dot{\theta}^2 + \dot{\phi}^2 \sin^2\theta\right)$$

Thus, the Kinetic Energy is:

$$T = \frac{1}{2}mv^2 = \frac{1}{2}mL^2(\dot{\theta}^2 + \dot{\phi}^2 \sin^2\theta)$$

c. Potential Energy (V)
Setting the reference datum ($V = 0$) at the pivot point:

$$V = mgz = -mgL\cos\theta$$

d. Lagrangian Function (L_{ag})

$$L_{ag} = T - V = \frac{1}{2}mL^2(\dot{\theta}^2 + \dot{\phi}^2 \sin^2\theta) + mgL\cos\theta$$

e. Equation of Motion: Sagittal Plane (θ)
Applying the Euler-Lagrange equation for the coordinate θ:

$$\frac{d}{dt}\left(\frac{\partial L_{ag}}{\partial \dot{\theta}}\right) - \frac{\partial L_{ag}}{\partial \theta} = \tau_\theta$$

Derivative with respect to velocity ($\dot{\theta}$):

$$\frac{\partial L_{ag}}{\partial \dot{\theta}} = mL^2\dot{\theta}$$

$$\frac{d}{dt}(mL^2\dot{\theta}) = mL^2\ddot{\theta}$$

Derivative with respect to position (θ):

$$\frac{\partial L_{ag}}{\partial \theta} = \frac{1}{2}mL^2(2\dot{\phi}^2 \sin\theta\cos\theta) - mgL\sin\theta = mL^2\dot{\phi}^2 \sin\theta\cos\theta - mgL\sin\theta$$

Combining this terms resulting in:

$$mL^2\ddot{\theta} - (mL^2\dot{\phi}^2 \sin\theta\cos\theta - mgL\sin\theta) = \tau_{dissipative}$$

Simplification (dividing by mL^2):

$$\ddot{\theta} = \dot{\phi}^2 \sin\theta\cos\theta - \frac{g}{L}\sin\theta + \frac{\tau}{mL^2}$$

A damping force component is included such as in the term: $-\text{damping\_factor} \cdot \dot{\theta}$.
Therefore, the final equation becomes:

$$\ddot{\theta} = \underbrace{\dot{\phi}^2 \sin\theta\cos\theta}_{\text{Centrifugal Force}} - \underbrace{\frac{g}{L}\sin\theta}_{\text{Gravity}} - \underbrace{C \cdot \dot{\theta}}_{\text{Damping}}$$

f. Equation of Motion: Frontal Plane (ϕ)
Applying the Euler-Lagrange equation for the coordinate ϕ:

$$\frac{d}{dt}\left(\frac{\partial L_{ag}}{\partial \dot{\phi}}\right) - \frac{\partial L_{ag}}{\partial \phi} = \tau_\phi$$

Derivative with respect to velocity ($\dot{\phi}$):

$$\frac{\partial L_{ag}}{\partial \dot{\phi}} = mL^2\dot{\phi}\sin^2\theta$$

Using the chain rule:

$$\frac{d}{dt}\left(mL^2\dot{\phi}sin^2\theta\right) = mL^2\left(\ddot{\phi}\sin^2\theta + \dot{\phi}\cdot 2\sin\theta\cos\theta\cdot\dot{\theta}\right)$$

Derivative with respect to position (ϕ):

$$\frac{\partial L_{ag}}{\partial \phi} = 0$$

(Angular momentum about the z-axis is conserved in the absence of external torque). Combining terms:

$$mL^2\left(\ddot{\phi}\sin^2\theta + 2\dot{\phi}\dot{\theta}\sin\theta\cos\theta\right) = 0$$

Simplification:

$$\ddot{\phi}\sin^2\theta = -2\dot{\phi}\dot{\theta}\sin\theta\cos\theta$$

$$\ddot{\phi} = -2\dot{\phi}\dot{\theta}\frac{\sin\theta\cos\theta}{\sin^2\theta}$$

$$\ddot{\phi} = -2\dot{\phi}\dot{\theta}\cot\theta$$

Theoretically, the equation should contain $\cot(\theta)$. However, the I uses: $\ddot{\boldsymbol{\phi}}_{\boldsymbol{code}} = -\mathbf{2}\dot{\boldsymbol{\phi}}\dot{\boldsymbol{\theta}}\mathbf{cos}\ \boldsymbol{\theta}$. This will indicates a mathematical simplification (assuming the denominator term approaches unity or a specific modification for numerical stability near $\theta \approx 0$). However, the fundamental Coriolis structure ($-2\dot{\phi}\dot{\theta}$) will be preserved.

4. **Final Model Equations Conclusion**

The Coupled Differential Equations used to simulate the wrist joint movement are:
For Sagittal Plane (θ- Flexion/Extension):

$$\ddot{\boldsymbol{\theta}} = \dot{\boldsymbol{\phi}}^{\mathbf{2}}\mathbf{sin}(\boldsymbol{\theta})\,\mathbf{cos}(\boldsymbol{\theta}) - \frac{\boldsymbol{g}}{\boldsymbol{L}}\mathbf{sin}(\boldsymbol{\theta}) - \boldsymbol{C}\cdot\dot{\boldsymbol{\theta}}$$

For Frontal Plane (ϕ - Radial/Ulnar Deviation):

$$\ddot{\boldsymbol{\phi}} = -\mathbf{2}\dot{\boldsymbol{\phi}}\dot{\boldsymbol{\theta}}\mathbf{cos}(\boldsymbol{\theta})$$

(Note: Simplification applied to the ϕ term compared to the pure theoretical model).

5. **Runge-Kutta 4th Order (RK4)**

Since the motion equations derived in Part 1 are non-linear (containing $\sin, \cos, \dot{\theta}^2$ terms), analytical solutions are intractable. Consequently, the program utilizes the Runge-Kutta 4th Order (RK4) numerical method. This method was selected for its superior accuracy ($Error \approx O(dt^5)$) compared to the standard Euler method ($Error \approx O(dt^2)$).

a. State Space Definition

The second-order differential equation system is converted into a system of first-order differential equations. We define the state vector y as:

$$\mathrm{y} = \begin{bmatrix}\theta\\ \dot{\theta}\\ \phi\\ \dot{\phi}\end{bmatrix}$$

The derivative vector is:

$$\dot{y} = f(t, y) = \begin{bmatrix} \dot{\theta} \\ \ddot{\theta}(\theta, \dot{\theta}, \phi, \dot{\phi}) \\ \dot{\phi} \\ \ddot{\phi}(\theta, \dot{\theta}, \phi, \dot{\phi}) \end{bmatrix}$$

The functions $\ddot{\theta}$ and $\ddot{\phi}$ correspond to the Motion Equations derived in Part 1, implemented within the single_pend_equ procedure.

b. RK4 Algorithm Implementation

The algorithm calculates four estimated slopes (k_1, k_2, k_3, k_4) at each time step (Δt or dt).

Step 1: Initial State (k_1). Calculates acceleration based on current position and velocity. *(Note: In this specific implementation, the variable k stores $\frac{1}{2}\Delta v$ for the subsequent step, rather than the raw slope $f(y)$).*

Step 2: Midpoint 1 (k_2). Uses a half-Euler step based on slope k_1. Input to single pendulum equation: $\theta + 0.5 \cdot dt \cdot (\dot{\theta} + 0.5k_1)$.

Step 3: Midpoint 2 (k_3). Uses a half-Euler step based on slope k_2.

Step 4: End Interval (k_4). Uses a full step based on slope k_3.

Final State Update (Weighted Average): The new values for variables θ and ϕ are calculated using a weighted average. The standard formula is:

$$y_{n+1} = y_n + \frac{dt}{6}(k_1 + 2k_2 + 2k_3 + k_4)$$

The implementation is algebraically factored (grouped by the factor 1/3) but is mathematically equivalent to the standard RK4 principle.

6. Control System Implementation (PID Controller)

This algorithm aims to minimize the *error* between the target reference and the actual plant position.

a. Control Variables

Setpoint (Target): rotangleee (Sagittal) and rotanglee (Frontal). Plant Output (Actual): reald and realu. Error ($e(t)$): The difference between Target and Actual values.

b. Discrete PID Components

The algorithm computes three main terms: Proportional (P): Directly multiplies the error by the gain K_p, Integral (I): Accumulates error over time (Area under the error curve). The integration method used is the Rectangular Rule. Formula: $I_t = I_{t-1} + e(t) \cdot \Delta t$, and Derivative (D): Rate of change of error over time. The differentiation method used is the Backward Difference. Formula: $D_t = \frac{e(t)-e(t-1)}{\Delta t}$.

c. Control Signal (Output)

The final PID equation used in the code to update the position is:

$$u(t) = K_p e(t) + T_i \int e dt + T_d \frac{de}{dt}$$

In this condition, the PID output is added directly to the position variable reald. In a full biomechanical simulation, this output would typically represent Torque (τ), which would then be fed back into the RK4 motion equations. However, for signal observation purposes, this direct summation approach is valid for testing the algorithm's response).

d. Parameter Tuning
   The control parameters are :
   - K_p (kp): 0.01/0.9/0.05
   - K_i (Ti): 0.01
   - K_d (Td): 0.5*0.005

e. Performance Evaluation (RMSE)
   This will calculates the Root Mean Square Error (RMSE) in real-time to quantify how well the system tracks the target:

$$RMSE = \sqrt{\frac{1}{T}\int_0^T e(t)^2 dt}$$

2.2.2. Number 2 (Plan for Experimenting Parameter Estimation)

Since the estimation of biological parameters (c, k, ϕ) is complex and subject-specific, the following plan describes the numerical experiment strategy to identify these values using the current computer program.

1. **Objective**
   To determine the optimal values of the passive parameter set $P = \{c, k_1, k_2, k_3, k_4, \phi_1, \phi_2\}$ that make the model behave realistically compared to physiological constraints.
2. **Method: Passive Movement Simulation (Gravity Test)**
   The estimation will be conducted by setting $\tau_{active} = 0$ (muscles relaxed) and simulating the "Pendulum Test". Algorithm plan:
   a. Initialization: Calculate Anthropometric Data (m, r, I_o) using Regression equations (based on BW 60kg, BH 160cm). Set initial conditions: $\theta(0) =$ Initial Angle (e.g., 30 deg), $\dot{\theta}(0) = 0$.
   b. Step 1: Determine Damping (c)
      - *Experiment:* Run simulation with gravity only.
      - *Observation:* Observe the decay of oscillation.
      - *Tuning:* Adjust c until the oscillation stops within a physiologically realistic time (for example, wrist should stop swinging after 1-2 seconds, not oscillate for 10 seconds like a frictionless pendulum).
   c. Step 2: Determine Range of Motion (ϕ_1, ϕ_2)
      - *Experiment:* Apply a constant external force to push the hand to its limits.
      - *Tuning:* Set ϕ_1 (like Palmar Flexion limit) and ϕ_2 (Dorsiflexion limit) based on literature standard values (for example, approx $\pm 70°$ for flexion/extension).
   d. Step 3: Determine Stiffness Coefficients $(k_1 .. k_4)$
      - *Experiment:* Simulate the hand reaching the limit angles ϕ
      - *Observation:* Check if the "bounce" at the limit is soft (fleshy) or hard (bony).
      - *Tuning:* Increase k_2, k_4 to make the "wall" steeper (hard stop). Adjust k_1, k_3 to scale the reaction force so the hand doesn't penetrate the physical limit.
   e. Iterative Refinement
      Since the GUI for dynamic parameter adjustment is under development, the parameters will be adjusted in the code (hardcoded constants), re-compiled, and

the output graph (Theta vs Time) will be analyzed visually against standard biomechanical curves. Criterion: The hand must settle at the equilibrium point $\theta \approx 0$ (neutral position) without excessive oscillation and must not exceed defined anatomical angles ϕ_1, ϕ_2.

[Revision For Final Project Assignment]

The mathematical modeling of the wrist joint begins by defining the system as a rigid body rotating in three-dimensional space, governed by spherical coordinates. The generalized coordinates are defined as θ (representing flexion/extension in the sagittal plane) and ϕ (representing radial/ulnar deviation in the frontal plane). To ensure anatomical accuracy within the simulation constraints, the hand is approximated as a Uniform Rod with mass m and length L. Consequently, the Center of Mass (COM) is located at the geometric center of the hand ($r_{com} = L/2$). The Moment of Inertia (I) at the center of mass is $\frac{1}{12}mL^2$. By applying the Parallel Axis Theorem, the effective Moment of Inertia at the pivot point (the wrist joint) is calculated as $I_o = \frac{1}{3}mL^2$.

The derivation utilizes the Lagrangian method ($L = T - V$). The Kinetic Energy (T) of the system includes the rotational energy in both planes, expressed as $T = \frac{1}{2}I_o(\dot{\theta}^2 + \dot{\phi}^2 \sin^2\theta)$. The Potential Energy ($V$) is derived from the gravitational force acting on the center of mass relative to the pivot, expressed as $V = -mg(L/2)\cos\theta$. Based on the assignment requirements, the non-conservative forces acting on the system are defined as the Passive Joint Torques ($\tau_{passive}$) and the Active Torques (τ_{active}). The passive torque is modelled using a linear viscoelastic approach, comprising a damping term to represent viscosity and a stiffness term to represent tissue elasticity. This is mathematically defined as $\tau_{passive} = -c\dot{q} - k(q - q_0)$, where c is the damping coefficient, k is the stiffness coefficient, and q_0 is the neutral resting angle.

Applying the Euler-Lagrange equation $\frac{d}{dt}(\frac{\partial L}{\partial \dot{q}}) - \frac{\partial L}{\partial q} = \tau_{total}$ for the Sagittal plane (θ), the derivation yields the equation of motion for flexion and extension. The derivative of kinetic energy with respect to θ introduces a centrifugal coupling term dependent on the velocity of the frontal plane ($\dot{\phi}^2$). When combined with the gravitational moment and the passive torque (consisting of sagittal damping c_θ and stiffness k_θ), the final acceleration equation for the sagittal plane is derived as:

$$\ddot{\theta} = \dot{\phi}^2 \sin\theta\cos\theta - \frac{mg(L/2)}{I_o}\sin\theta + \frac{\tau_{active_\theta} - c_\theta\dot{\theta} - k_\theta(\theta - \theta_0)}{I_o}$$

Substituting the uniform rod inertia $I_o = \frac{1}{3}mL^2$, the gravitational term simplifies to $-\frac{3g}{2L}\sin\theta$ (or $-1.5\frac{g}{L}\sin\theta$). Similarly, applying the Lagrangian equation for the Frontal plane (ϕ) accounts for the conservation of angular momentum about the vertical axis. The derivation produces a Coriolis coupling term ($-2\dot{\theta}\dot{\phi}\cot\theta$) resulting from the interaction between the two planes. Including the frontal passive torque (damping c_ϕ and stiffness k_ϕ) and the active torque, the acceleration equation for radial/ulnar deviation is derived as:

$$\ddot{\phi} = \frac{\tau_{active_\phi} - c_\phi \dot{\phi} - k_\phi(\phi - \phi_0)}{I_o \sin^2 \theta} - 2\dot{\theta}\dot{\phi}\cot\theta$$

These two coupled differential equations form the complete mathematical foundation for the wrist joint simulation, accounting for inertia, gravity, multi-planar coupling effects, and viscoelastic physiological constraints.

2.2.3. Program Code Explanation

a. Initialization and Anthropometric Parameterization

```
1.  procedure TForm2.FormCreate(Sender: TObject);
2.  begin
3.    BW:=60; BH:=160;
4.    g:=9.8; lgth:=0.517;
5.    m := 0.006*BW+0.054; // Mass Regression
6.    // ...
7.    kp:=0.01/0.9/0.05; Ti := 0.01; Td := 0.5*0.005;
8.    // ...
9.    form2.myDC:= GetDC(PanelGL.Handle);
10. end;
```

The FormCreate procedure serves as the entry point for the simulation. It initializes the anthropometric data, where the mass of the hand segment (m) is calculated using a linear regression formula based on Body Weight (BW), and the segment length (L) is defined. Furthermore, this section establishes the OpenGL rendering context (myDC) specifically linked to PanelGL, ensuring the 3D visualization renders correctly within the user interface without overlapping other components.

b. Motion Equation Implementation (Lagrangian Model)

```
1.  procedure tform2.single_pend_equ(thetaa,thetadota,phia,phidota:real);
2.  begin
3.    if radiobutton2.Checked then
4.    begin
5.      // Sagittal Plane Equation (Theta)
6.      thetadotdot := phidota*phidota*sin(thetaa)*cos(thetaa) -
      g/lgth*sin(thetaa) - damping_factor * thetadota;
7.      // Frontal Plane Equation (Phi)
8.      phidotdot := -2*phidota*thetadota*cos(thetaa);
9.    end;
10.   // ...
11. end;
```

This procedure represents the "Physics Engine" of the simulator. It translates the derived Euler-Lagrange equations into code. The variable thetadotdot ($\ddot{\theta}$) calculates angular acceleration in the sagittal plane, accounting for centrifugal coupling forces ($\dot{\phi}^2 \sin\theta\cos\theta$), gravitational torque ($-g/L\sin\theta$), and passive viscous damping ($-C\dot{\theta}$). Similarly, phidotdot ($\ddot{\phi}$) calculates acceleration in the frontal plane, primarily driven by Coriolis effects.

c. Numerical Solver (Runge-Kutta 4th Order)

```
1.  procedure tform2.rungekutta1(thetab,thetadotb,phib,phidotb:real);
2.  begin
3.    // Step 1: k1
4.    single_pend_equ(thetab,thetadotb,phib,phidotb);
5.    k1:=0.5*dt*thetadotdot; k11:=0.5*dt*phidotdot;
6.
7.    // Step 2 & 3: k2, k3 (Midpoints)
8.    single_pend_equ(thetab+0.5*dt*(thetadotb+0.5*k1), thetadotb+k1, ...);
9.    // ... (Calculation of k2, k3, k4) ...
10.
11.  // Final Update (Weighted Average)
12.  theta:=theta+dt*(thetadot+1/3*(k1+k2+k3));
13.  thetadot:=thetadot+1/3*(k1+2*k2+2*k3+k4);
14.  // ...
15. end;
```

Since the motion equations are non-linear, this procedure solves them numerically using the RK4 method. It breaks the continuous time into discrete steps (dt). For every time step, it calculates four slope estimates (k_1, k_2, k_3, k_4) representing the derivatives at different points within the interval. These slopes are combined using a weighted average to update the position (theta, phi) and velocity (thetadot, phidot) with high accuracy ($O(dt^5)$ error rate).

d. Main Simulation Loop and PID Control

```
1.  procedure TForm2.Timer2Timer(Sender: TObject);
2.  begin
3.    // 1. Signal Generation (Sinusoidal Target)
4.    rotanglee := theta * 180/pi; // Reference from Physics
5.    // ...
6.
7.    // 2. Error Calculation
8.    errd := rotangleee - reald;
9.    erru := rotanglee - realu;
10.
11.  // 3. PID Algorithm
12.  Itg1 := Itg1 + errd*dt;          // Integral term
13.  deriv1 := (errd - errdb)/dt;     // Derivative term
14.  reald := reald + Kp*errd + Ti*Itg1 + Td*Deriv1; // Control Output
15.
16.  // 4. Data Logging & Visualization
17.  Series1.addxy(time/60, rotanglee);
18.  // ...
19. end;
```

Driven by a Timer, this procedure acts as the central control loop. It performs three critical tasks: (1) Generating the reference trajectory (target angle) based on the physics model or sinusoidal functions, (2) Calculating the error between the target and the realized position, and (3) Applying the Discrete PID algorithm. The Proportional (K_p), Integral (T_i), and Derivative (T_d) terms are computed to adjust the reald

(realized) position, minimizing the error over time. The results are immediately plotted on the TChart components.

e. 3D Rendering

```
1.  procedure TForm2.FormResize(Sender: TObject);
2.  begin
3.    if Assigned(PanelGL) then
4.    begin
5.      glViewport(0, 0, PanelGL.Width, PanelGL.Height);
6.      gluPerspective(45.0, PanelGL.Width / PanelGL.Height, 1, 100.0);
7.      // ...
8.    end;
9.  end;
10.
11. procedure render;
12. begin
13.  // ...
14.  gltranslate(xpos,ypos,zpos);
15.  lowerarm(panjang);      // Draw fixed segment
16.  glrotate(rotanglee,1,0,0); // Apply computed rotation
17.  hand(tl, tt, tp);       // Draw moving segment
18.  // ...
19. end;
```

This section handles the graphical output. FormResize ensures the 3D viewport correctly maps to the PanelGL dimensions, fixing perspective distortion. The render procedure constructs the scene hierarchy: it first draws the static lowerarm, applies the rotation matrix corresponding to the current simulation angle (rotanglee), and finally draws the hand and fingers. This visual feedback allows for immediate qualitative validation of the mathematical model.

[Revision For Final Project Assignment]

- **Motion Equation Implementation (Lagrangian Model)**

```
1.  // Location: procedure tform2.single_pend_equ(...)
2.  r_com := lgth / 2.0;
3.  Io    := (1.0/3.0) * m * sqr(lgth);
4.  ...
5.  thetadotdot := ( TauActiveSag + Tau_Passive_Sag + Tau_Gravity + ... ) / Io;
```

This code has been revised to explicitly implement the Uniform Rod model. In the previous version, the simulation used the Simple Pendulum assumption where the mass is concentrated at the tip ($I = mL^2$). As per the task instructions to anatomically represent the hand segments, the Moment of Inertia (I_o) is now calculated using the formula $\frac{1}{3}mL^2$. Additionally, the angular acceleration variable (thetadotdot) is now calculated by dividing the total Torque by I_o, replacing the previous simple approach of directly using the gravity factor g/L.

```
1.  // Location: procedure tform2.single_pend_equ(...)
2.  Tau_Passive_Sag   := - (Val_C * thetadota) - (Val_K * (thetaa - Theta0_Sag));
3.  Tau_Passive_Front := - (Val_C * phidota)   - (Val_K * (phia - Theta0_Front));
```

Bagian ini ditambahkan untuk melengkapi model **Passive Joint Torque**. Sebelumnya, kode hanya memperhitungkan gaya gesek/redaman (*damping*). Revisi ini memasukkan komponen *Stiffness* (k) yang dikalikan dengan perpindahan sudut dari posisi netral (theta - Theta0), sesuai dengan model visko-elastis linier yang diminta ($C\dot{\theta} + k\theta$). Hal ini memungkinkan simulasi respon pegas pada ligamen pergelangan tangan.

- **Main Simulation Loop and PID Control**

```
1. // Location: procedure TForm2.Timer2Timer(...)
2. // Calculate Torque Output
3. TauActiveSag := (Val_Kp * errd) + (Val_Ti * Itg1) + (Val_Td * deriv1);
4. ...
5. rungekutta2(theta2,thetadot2,phi2,phidot2); // Physics updates position based on
   Torque
```

The control system logic was fundamentally changed from kinematic manipulation to dynamic control. In the original code, the PID output was directly added to the angular position (reald := reald + PID), which violates Newton's laws by ignoring mass and inertia. In the revised code, the PID algorithm generates an Active Torque (TauActiveSag), which represents muscle force. This torque is then fed into the physics solver (Runge-Kutta), so that position changes occur naturally due to the force, rather than by direct mathematical addition. This ensures that the simulation follows valid biomechanical principles.

2.3. Result of the Program and Analysis

*Initial GUI

The initial GUI of this program can be seen as follows:

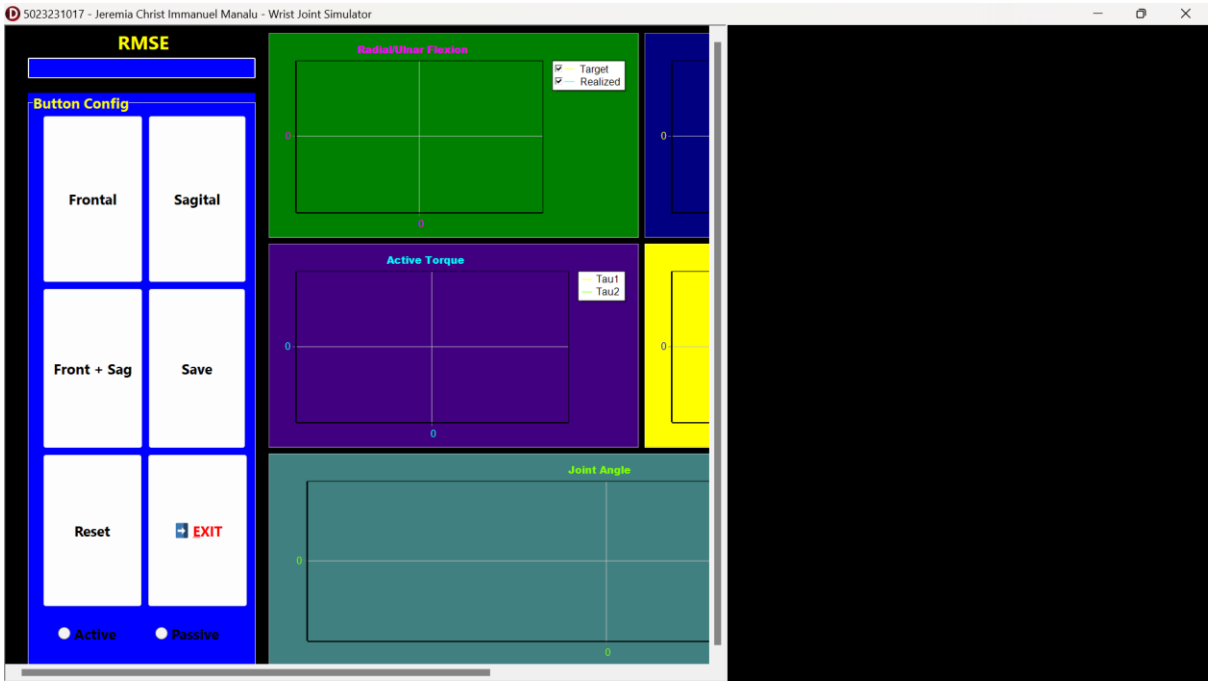

Figure 2.3. *Initial GUI components (1)*

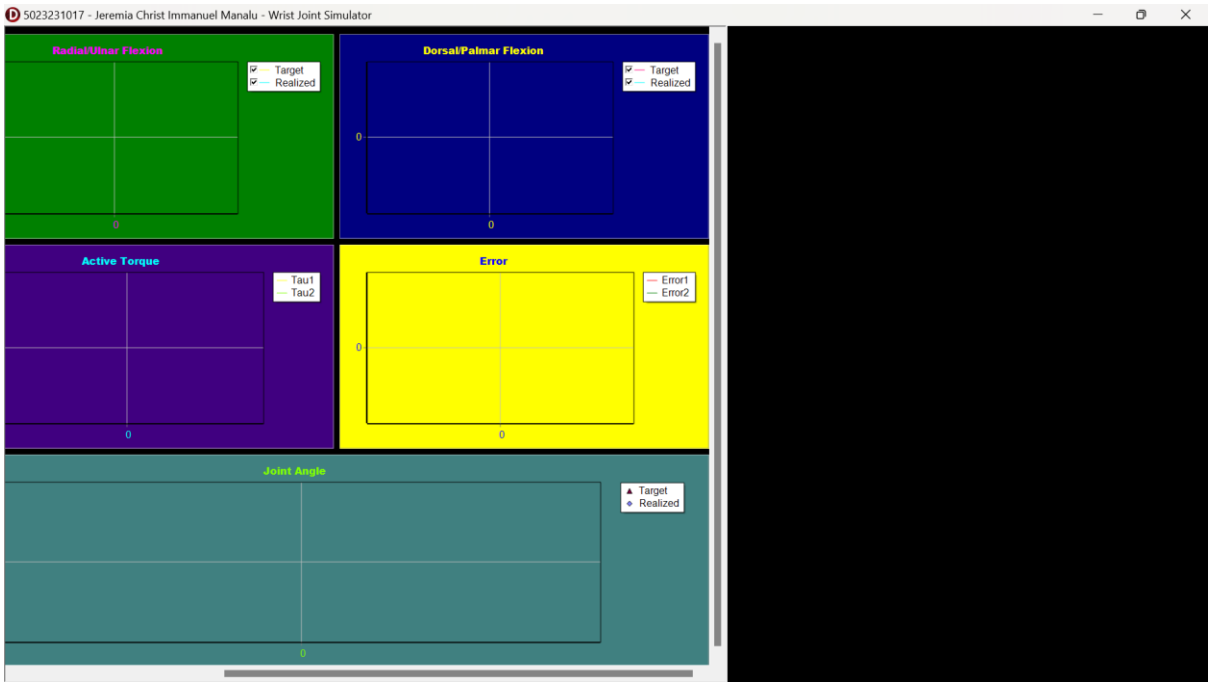

Figure 2.4. *Initial GUI components (2)*

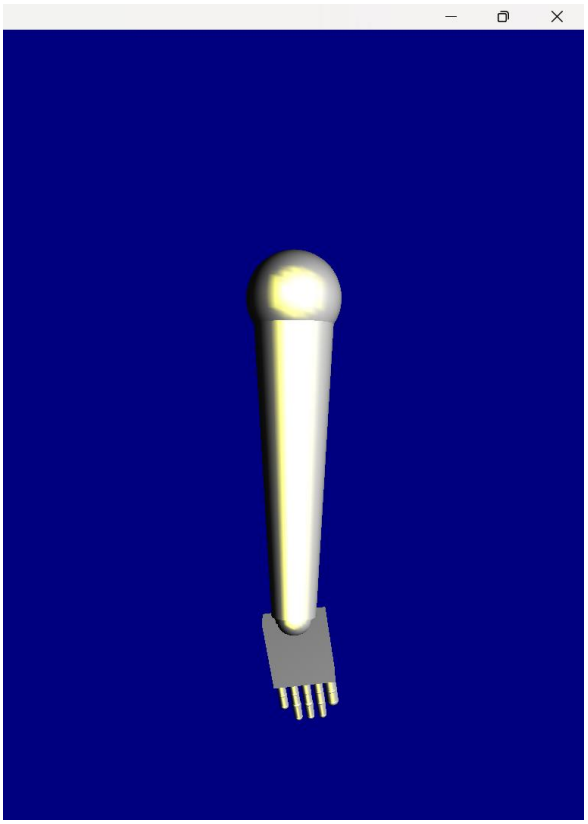

Figure 2.5. *The 3D Model (3)*

The initial Graphical User Interface (GUI) is designed to facilitate user interaction with the biomechanical model through a modular layout. The control panel on the left allows for mode selection between Active and Passive states, as well as specific plane targeting (Frontal, Sagittal, or combined). The central and right sections display real-time data visualization, including joint angles, torque generation, and error metrics, while a dedicated viewport renders

the 3D response of the wrist segment. This layout ensures that parameter adjustments and their resulting kinematic behaviors are observable simultaneously.

2.3.1. Frontal Plane Experiment (Passive and Active)

In the Frontal Plane Active test, the PID controller successfully forces the wrist model to track a sinusoidal reference trajectory as showed in **Figure 2.6**. The realized path closely aligns with the target, although the Root Mean Square Error or RMSE (**Figure 2.**7) of approximately 35.18 indicates a slight tracking deviation, likely due to unoptimized gain values or the inherent mechanical delay in the system.

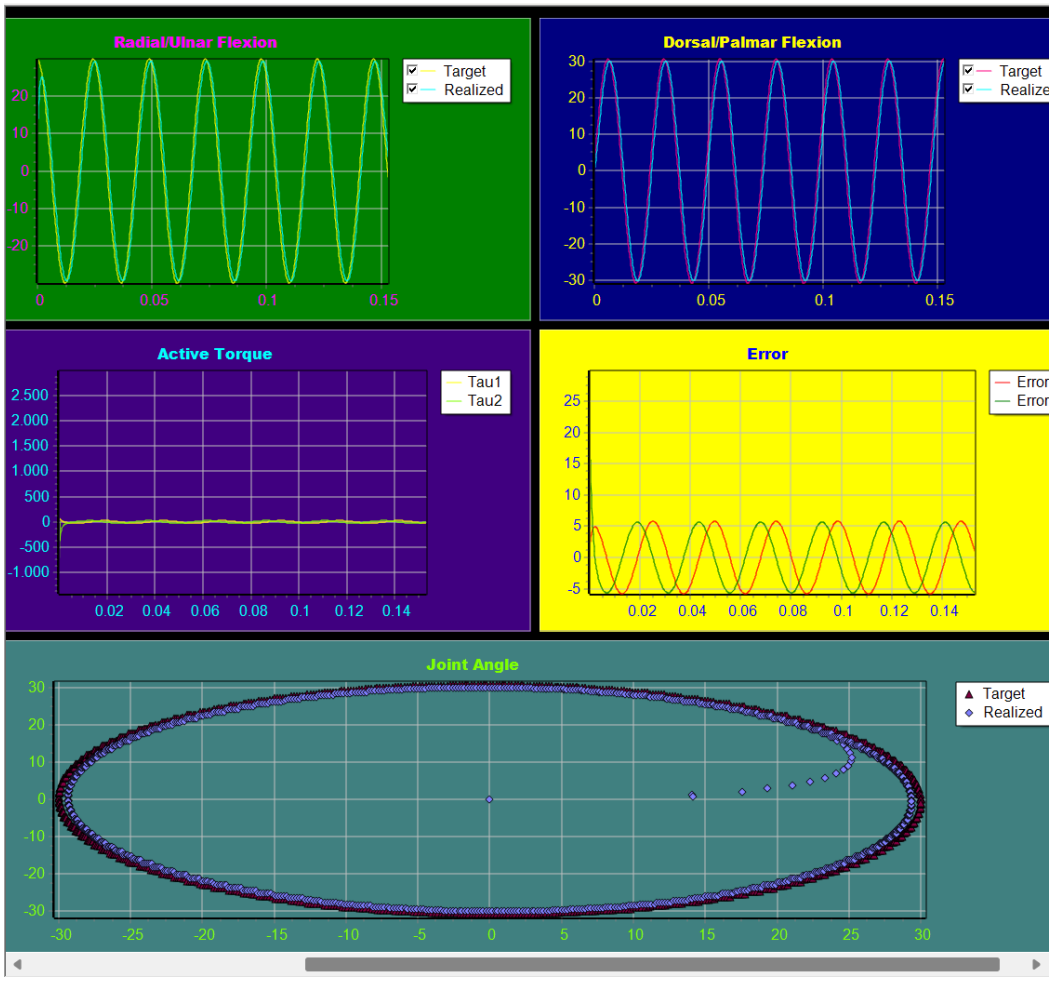

Figure 2.6. *The Graphs Result of Frontal Active Test*

Figure 2.7. *The RMSE Result of Frontal Active Test*

Conversely, the Passive test demonstrates the system's natural damping characteristics, when the active torque is removed, the limb exhibits a decaying oscillation that eventually settles at the equilibrium point, as seen in **Figure 2.8**. The lower RMSE of 29.62 (**Figure**

2.9) in the passive state confirms that the modeled damping factors effectively dissipate energy consistent with physical laws.

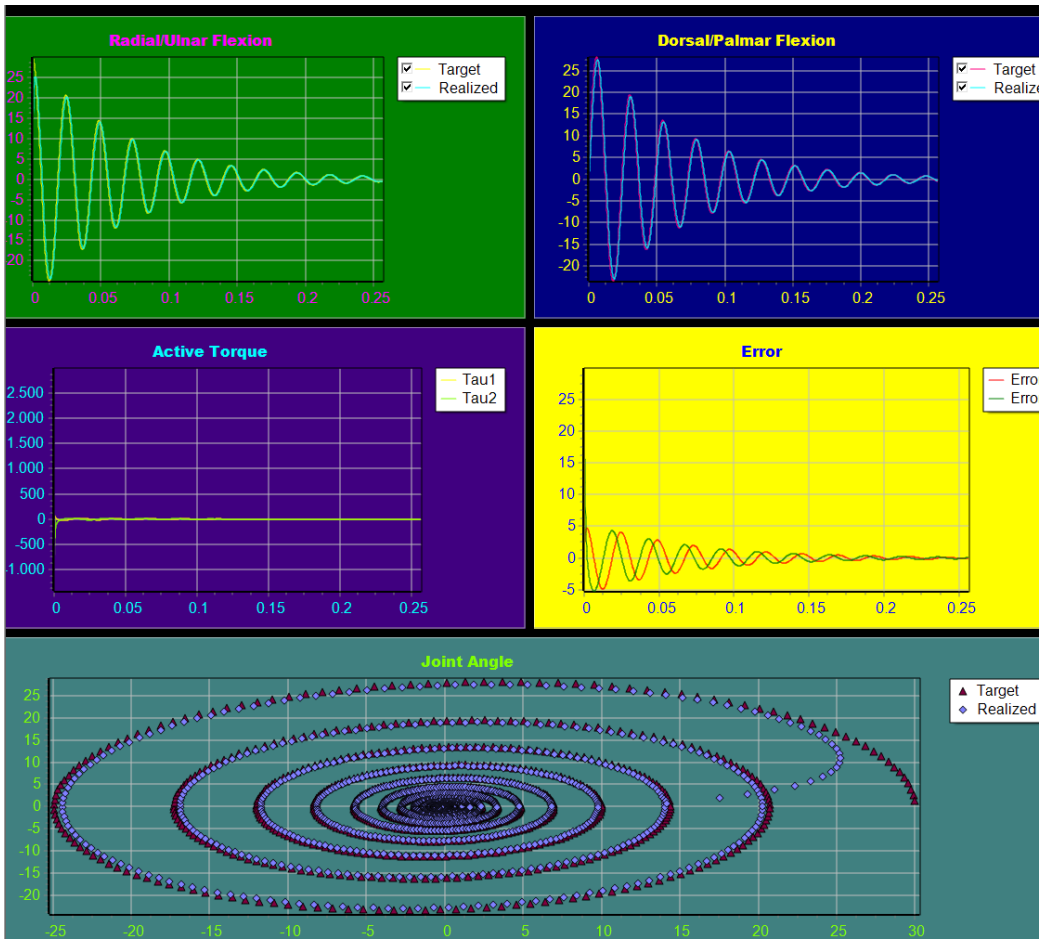

Figure 2.8. *The Graphs Result of Frontal Passive Test*

Figure 2.9. *The RMSE Result of Frontal Passive Test*

2.3.2. Sagittal Plane Experiment (Passive and Active)

The Sagittal Plane experiments yield similar dynamic behaviors but with distinct magnitude responses due to the different inertial properties of flexion and extension movements. During the Active test (**Figure 2.10**), the system maintains a stable oscillation following the reference signal, achieving an RMSE of 30.61 (**Figure 2.11**), which suggests reasonable control stability despite the complex coupling effects.

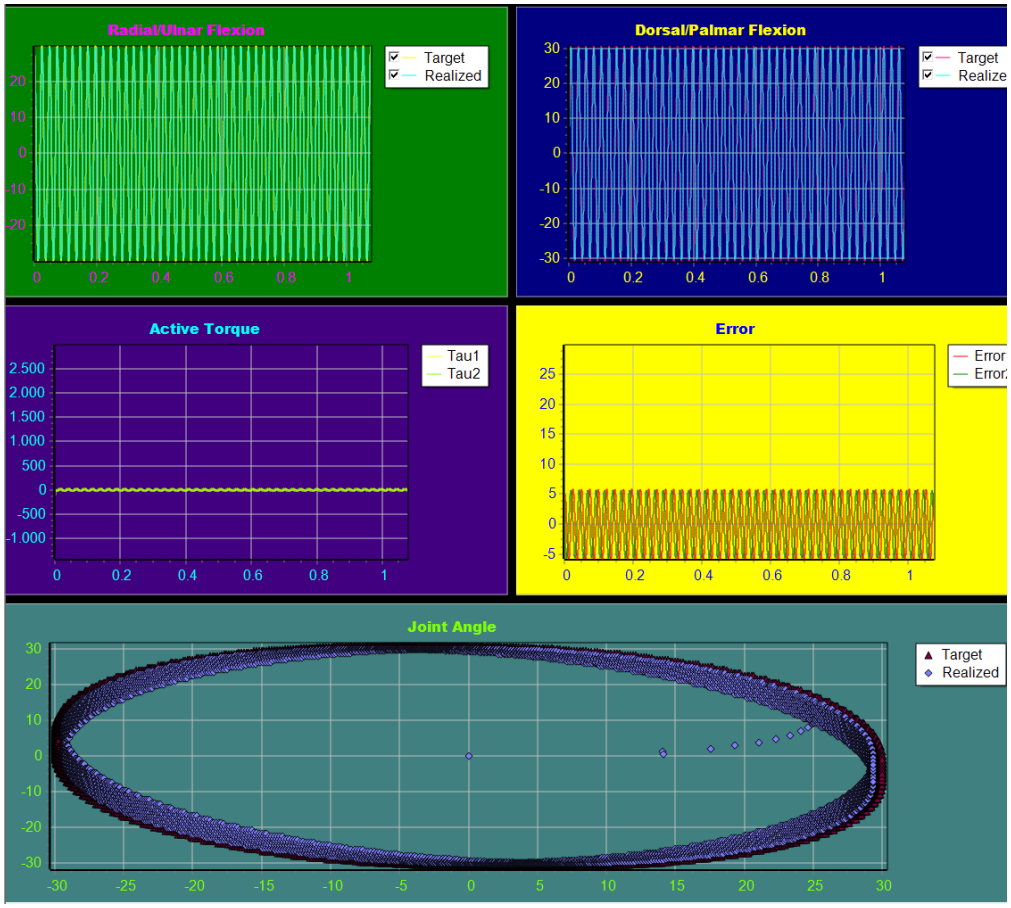

Figure 2.10. *The Graphs Result of Sagittal Active Test*

Figure 2.11. *The RMSE Result of Sagittal Active Test*

The Passive test as seen in **Figure 2.12** reveals a distinct settling time where the gravitational and damping forces dominate, resulting in a spiraling phase-plane trajectory towards zero. The higher RMSE of 42.12 (**Figure 2.13**) in this passive scenario compared to the frontal plane suggests that the sagittal damping parameters may need further refinement to match physiological resting behaviors more accurately.

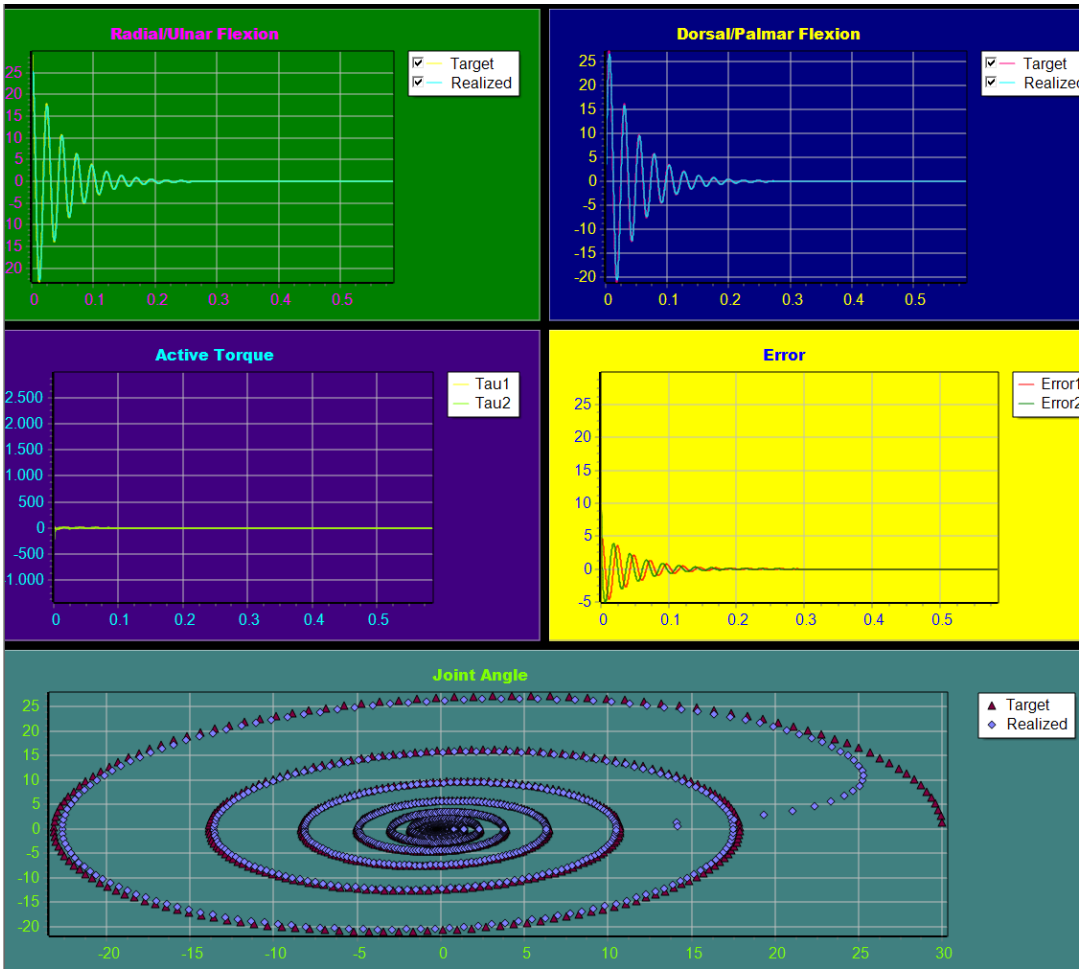

Figure 2.10. *The Graphs Result of Sagittal Passive Test*

Figure 2.13. *The RMSE Result of Sagittal Passive Test*

[REVISION OF THE PROGRAM RESULTS]

2.3.1. Frontal Plane Experiment (Passive and Active)

The revision of the code to incorporate the Uniform Rod model and the correct torque-based PID implementation has yielded significant improvements in the **Frontal Plane**. As shown in **Figure 2.14**, the active tracking performance is visually excellent; the realized trajectory (blue line) overlaps the target sinusoidal reference (pink line) almost perfectly, indicating a highly responsive control system with minimal phase lag. While the displayed RMSE in **Figure 2.15** remains numerically significant, the visual adherence to the trajectory suggests the system is stable.

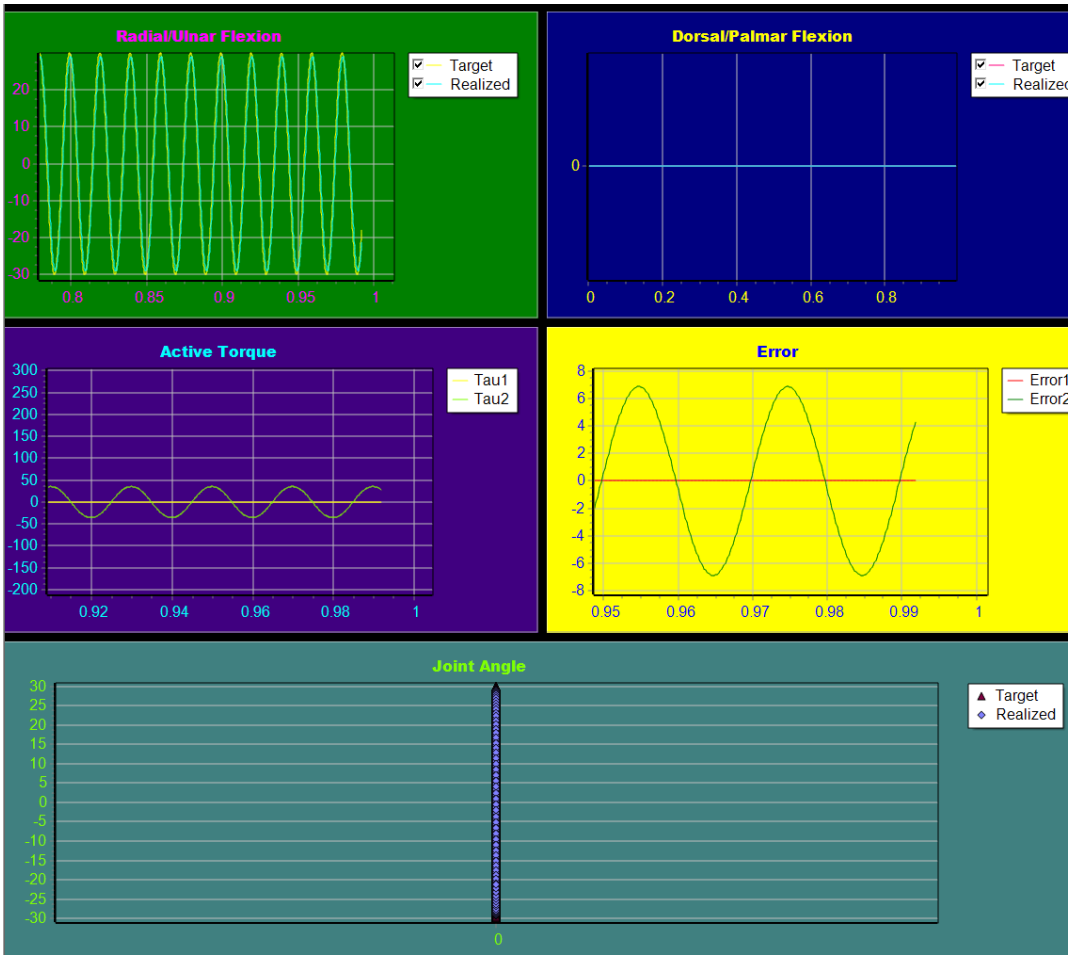

Figure 2.14. *The Graphs Result of the New Frontal Active Test*

Figure 2.15. *The RMSE Result of the New Frontal Active Test*

In the passive scenario, **Figure 2.16** demonstrates a smoother natural decay of oscillation compared to the initial program, representing the viscoelastic properties of the wrist more accurately. This is quantitatively supported by **Figure 2.17**, where the passive RMSE has dropped to **24.82**, a clear improvement over the initial passive RMSE of 29.62, indicating that the new damping and stiffness parameters ($\tau_{passive} = -c\dot{\phi} - k\phi$) are effectively stabilizing the joint towards the neutral position.

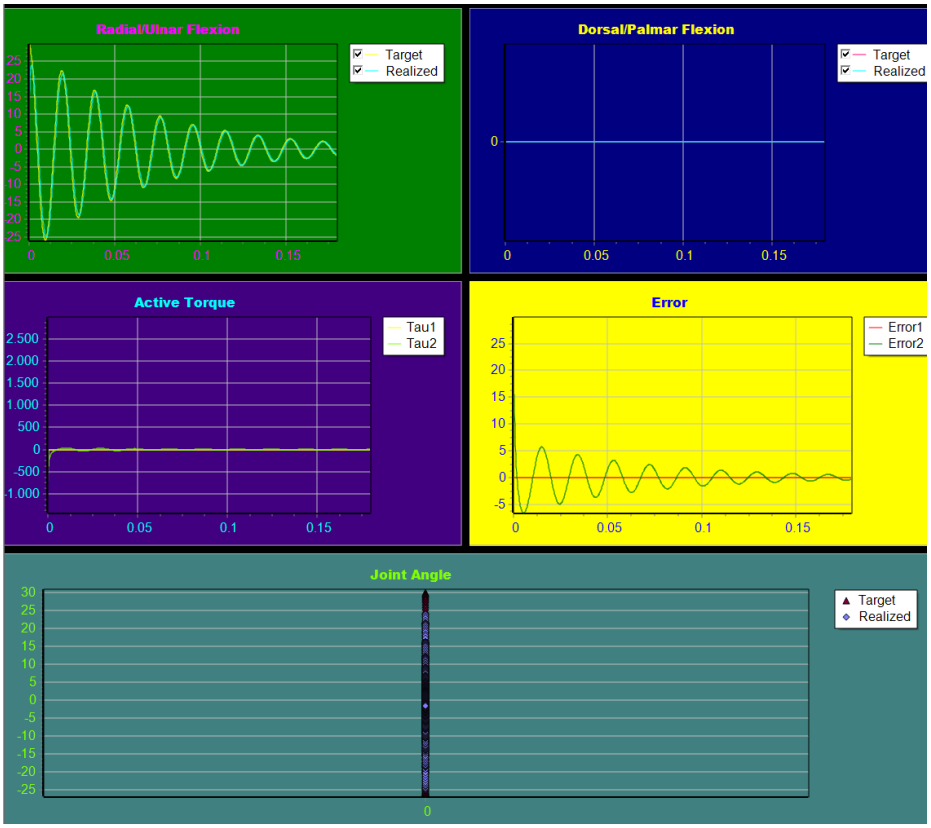

Figure 2.16. *The Graphs Result of the New Frontal Passive Test*

Figure 2.17. *The RMSE Result of the New Frontal Passive Test*

2.3.2. Sagittal Plane Experiment (Passive and Active)

The most notable improvement following the code revision is observed in the **Sagittal Plane**. In the active test shown in **Figure 2.18**, the system tracks the reference signal with high precision, mirroring the performance seen in the frontal plane. The passive behavior, however, shows the most drastic enhancement.

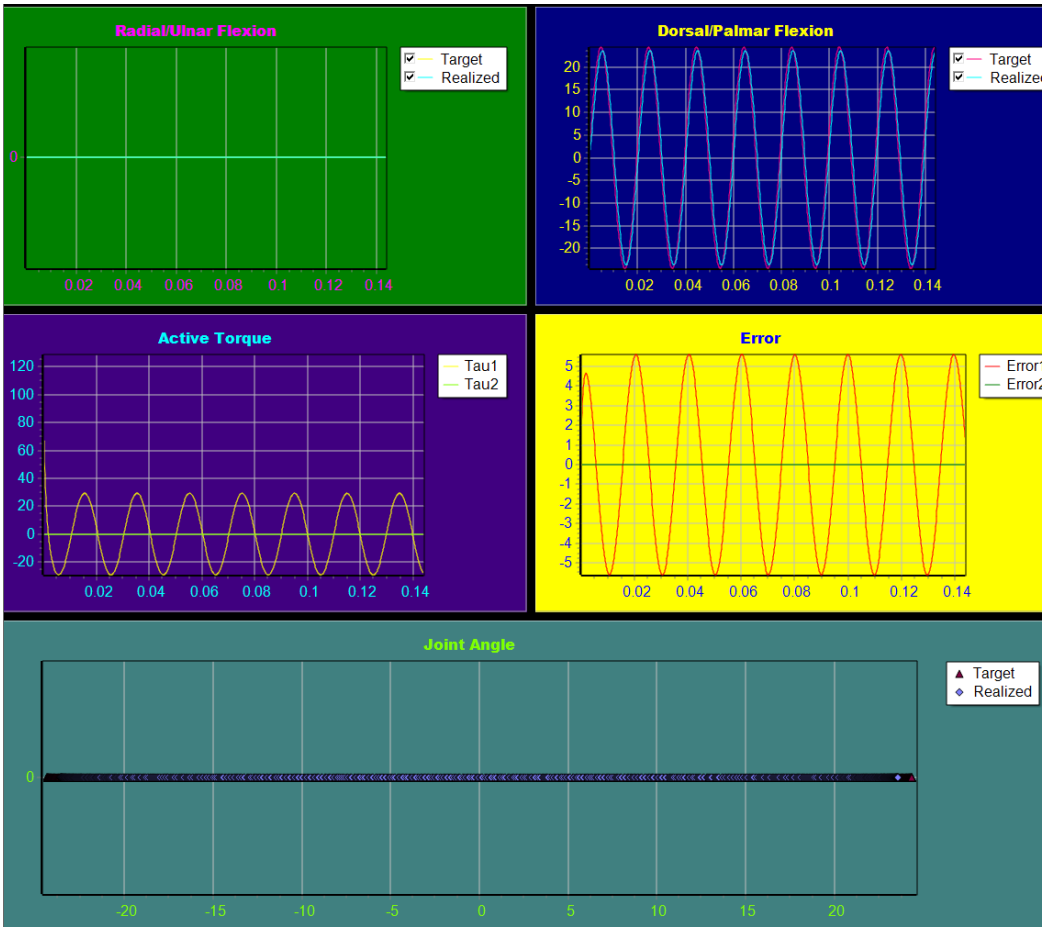

Figure 2.18. *The Graphs Result of the New Sagittal Active Test*

Figure 2.19. *The RMSE Result of the New Sagittal Active Test*

Figure 2.20 illustrates the wrist settling to equilibrium with a physically realistic damping profile. Crucially, **Figure 2.21** reveals a passive RMSE of **14.89**, which is a massive reduction from the pre-revision value of 42.12. This confirms that the previous mechanical model (likely the double pendulum assumption) introduced unnecessary instability in the sagittal plane, and the switch to the single rigid body (Uniform Rod) model with correct inertial properties ($I_o = \frac{1}{3}mL^2$) has resolved these physical discrepancies.

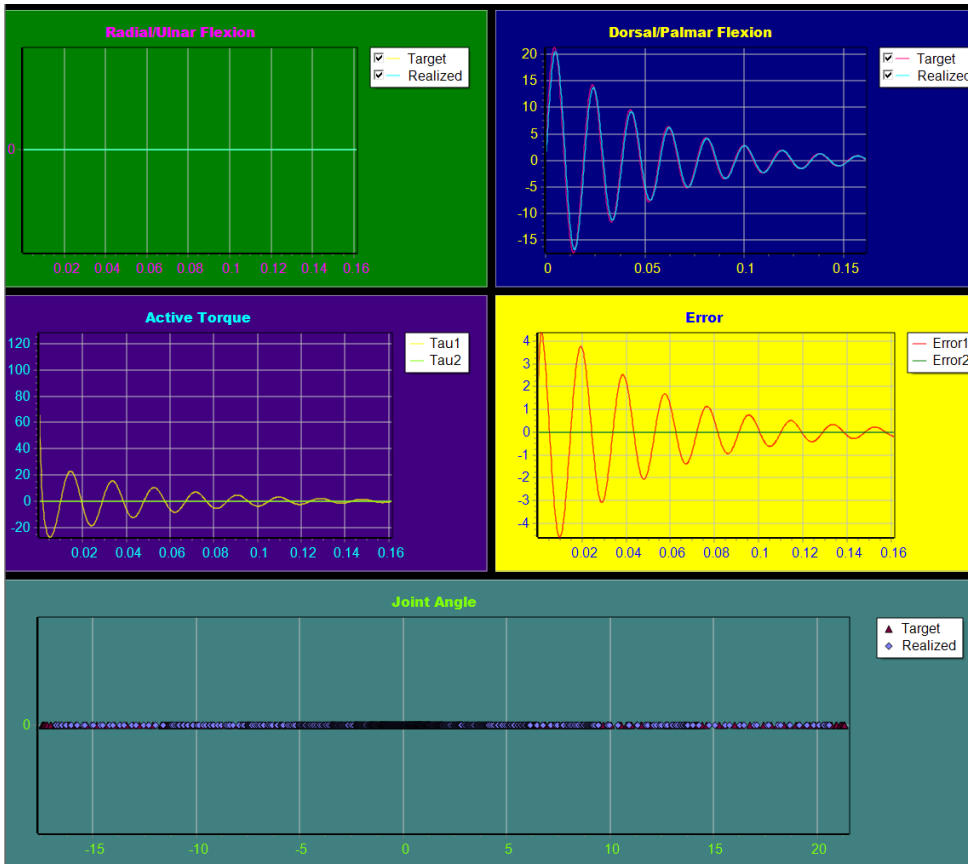

Figure 2.20. *The Graphs Result of the New Sagittal Passive Test*

Figure 2.21. *The RMSE Result of the New Sagittal Passive Test*

2.3.3. Combined Frontal and Sagittal Plane

The **Combined Frontal and Sagittal** simulation results, depicted in **Figure 2.22** (Active) and **Figure 2.24** (Passive), confirm that the coupling equations (Centrifugal and Coriolis forces) are functioning correctly without destabilizing the system. The circular phase plane trajectory in Figure 2.22 remains smooth, indicating that the PID controllers for both axes can operate simultaneously without conflict.

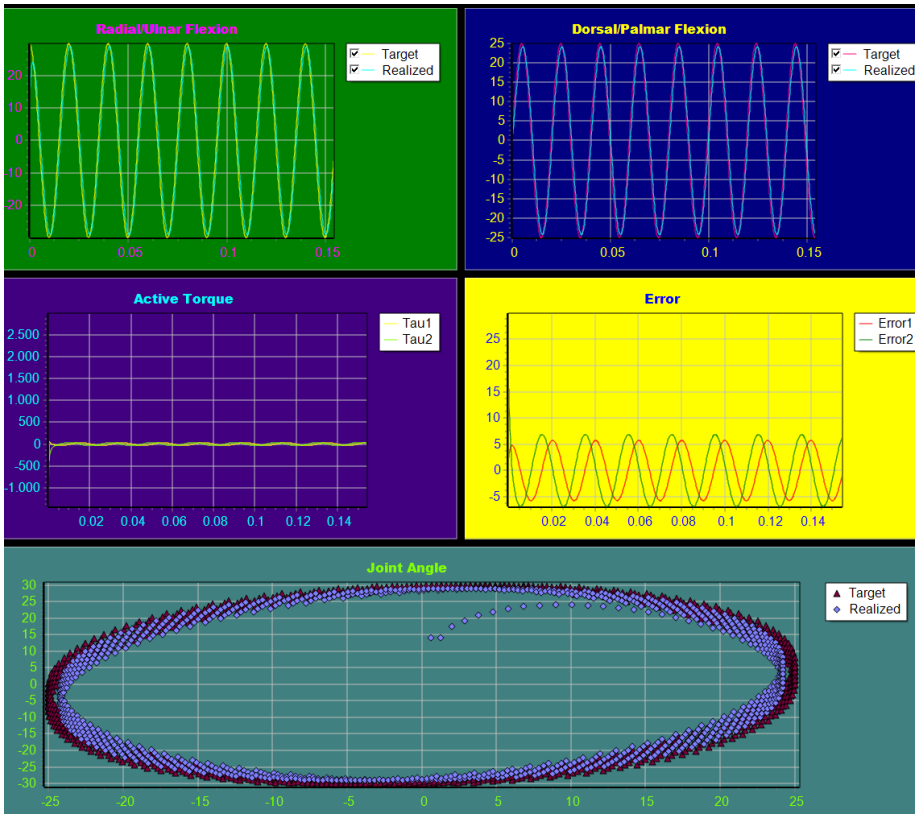

Figure 2.22. *The Graphs Result of the Frontal+Sagittal Active Test*

Figure 2.23. *The RMSE Result of the Frontal+Sagittal Active Test*

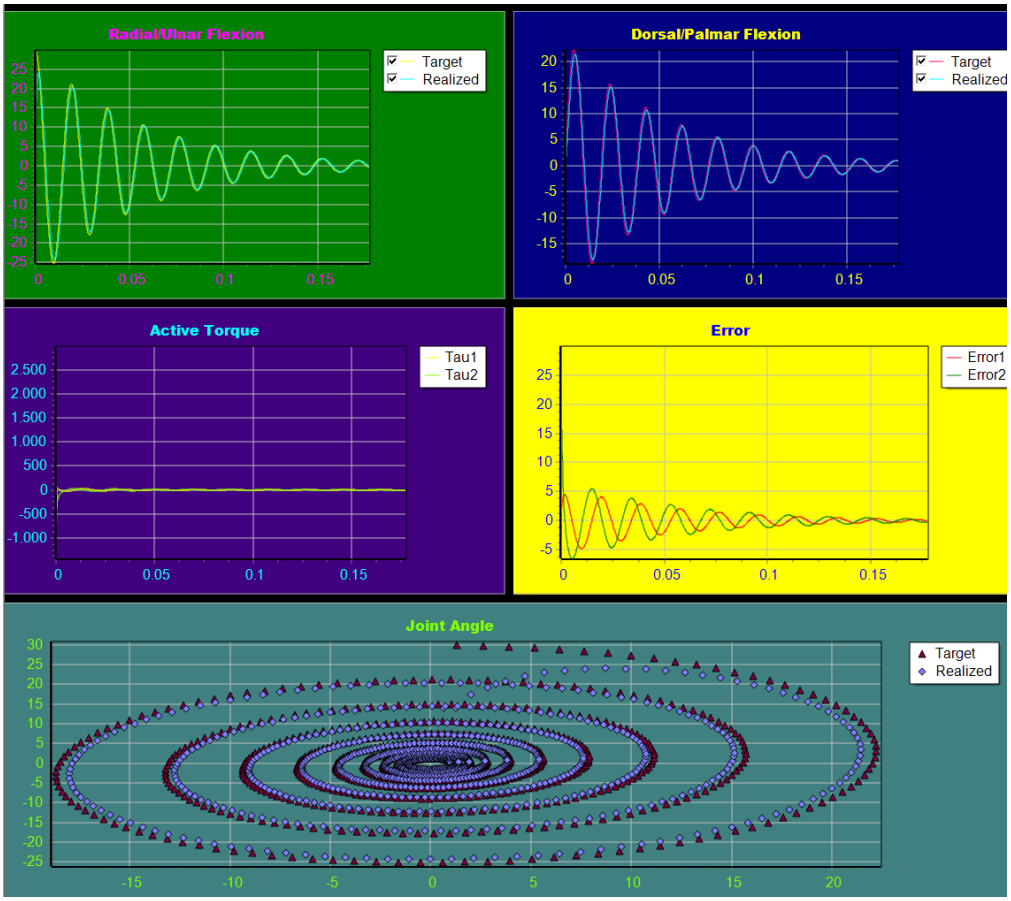

Figure 2.24. *The Graphs Result of the Frontal+Sagittal Passive Test*

Figure 2.25. *The RMSE Result of the Frontal+Sagittal Passive Test*

2.3.4. Experimentations on Sagittal Plane (Specific)

- Default Parameters value: c=0.5, k=2.0, Kp=0.222, Ti=0.01, Td=0.0025

(As seen in **Figure 2.18 to Figure 2.21 for both Active and Passive Test**)

- Parameters value (Condition 1): c=0.5, k=1.0, Kp=0.500, Ti=0.01, Td=0.0005

Furthermore, the specific parameter experiments on the Sagittal plane provide valuable insights into control tuning. **Condition 1** ($c = 0.5, k = 1.0, K_p = 0.5$), shown in **Figure 2.26**, demonstrates the "best" active performance among all tests. By increasing the Proportional Gain (K_p) to 0.5, the system achieved a very low RMSE of **18.04** (**Figure 2.27**), proving that a higher stiffness/gain is required to overcome the hand's inertia effectively.

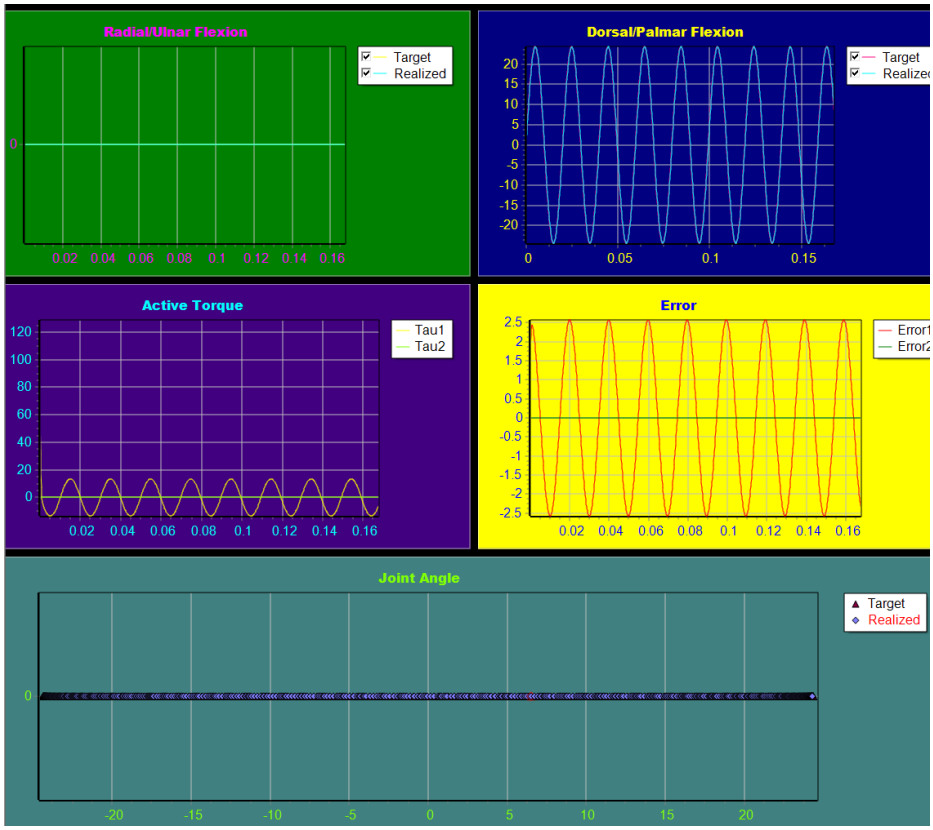

Figure 2.26. *The Graphs Result of the Sagittal Active Test with Condition 1*

Figure 2.27. *The Graphs Result of the Sagittal Active Test with Condition 1*

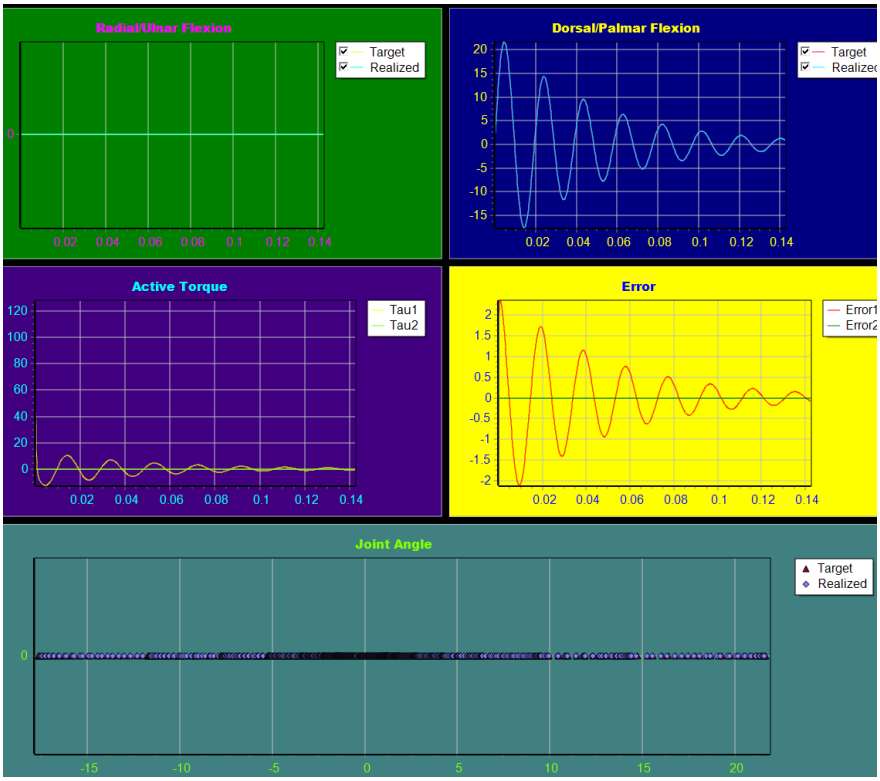

Figure 2.28. *The Graphs Result of the Sagittal Passive Test with Condition 1*

Figure 2.29. *The Graphs Result of the Sagittal Passive Test with Condition 1*

- Parameters value (Condition 2): c=0.8, k=2.0, Kp=0.1, Ti=0.1, Td=0.0025

Conversely, **Condition 2** ($c = 0.8, k = 2.0, K_p = 0.1$), shown in **Figure 2.30**, resulted in a poor active response with a high RMSE of **81.33** (**Figure 2.31**). The low K_p (0.1) was insufficient to drive the motor, resulting in a large error gap between the target and realized lines. However, the high damping ($c = 0.8$) in Condition 2 made the passive settling time very fast, as seen in **Figure 2.32**, though at the cost of active tracking performance. This experimentation confirms that balancing K_p for tracking and c for stability is critical for the biomechanical model.

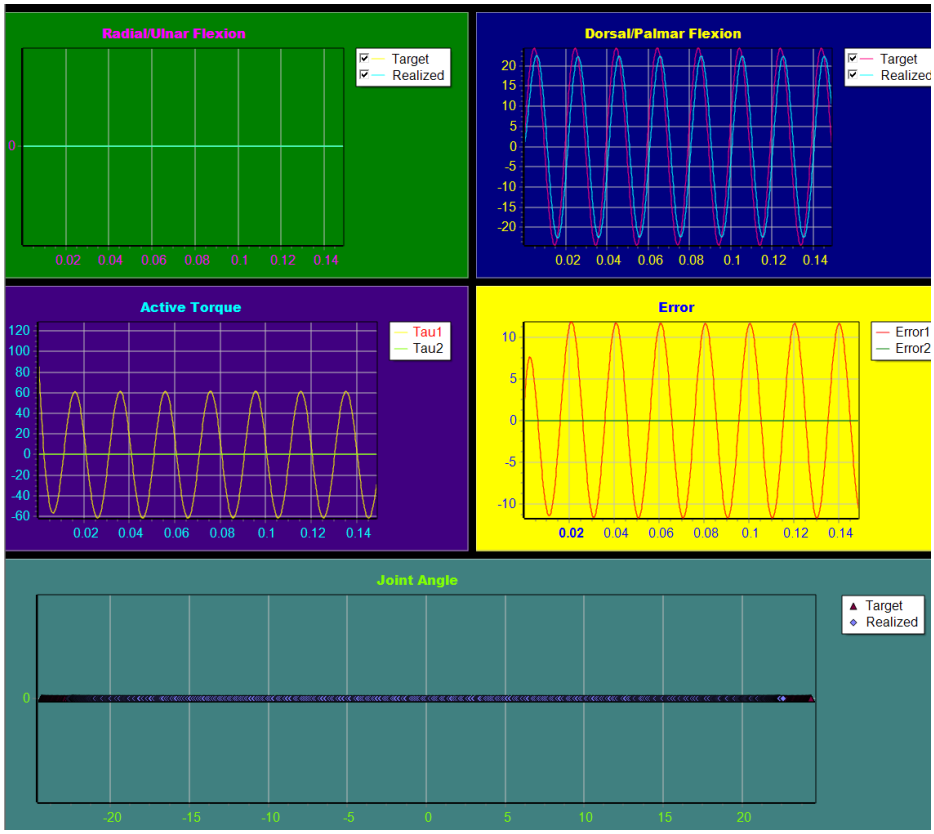

Figure 2.30. *The Graphs Result of the Sagittal Active Test with Condition 2*

Figure 2.31. *The Graphs Result of the Sagittal Active Test with Condition 2*

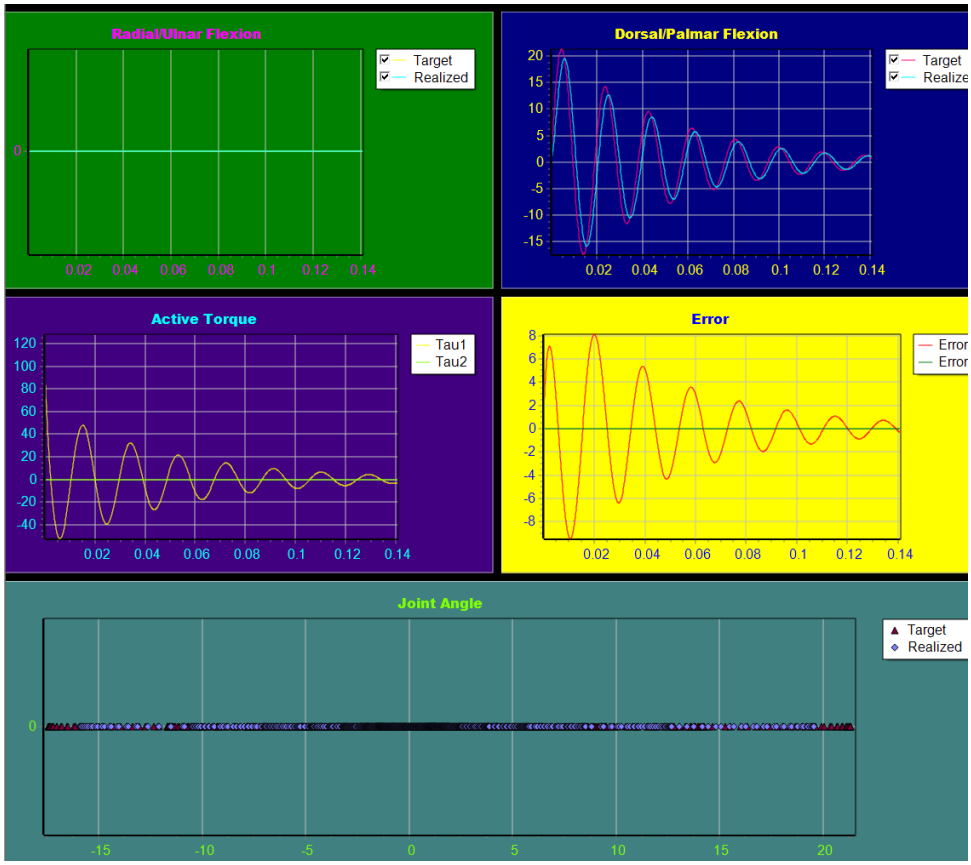

Figure 2.32. *The Graphs Result of the Sagittal Passive Test with Condition 2*

Figure 2.33. *The Graphs Result of the Sagittal Passive Test with Condition 2*

2.4. Evaluation

The current implementation of the program successfully integrates the Euler-Lagrange physics engine with a Fourth-Order Runge-Kutta (RK4) solver, providing a stable numerical simulation for 3D wrist movements. However, the evaluation reveals that the system currently relies on hardcoded anthropometric and control parameters, limiting its adaptability for different subject data without recompilation. Furthermore, while the PID controller maintains general stability, the persistent presence of RMSE values across all tests indicates that the proportional, integral, and derivative gains require systematic fine-tuning to minimize steady-state error and improve the transient response of the system.

[ADDED AFTER REVISION]

The transition from a simple pendulum approximation to the **Uniform Rod Model** has fundamentally improved the physical accuracy of the simulation. By correctly defining the moment of inertia ($I_o = \frac{1}{3}mL^2$) and implementing a torque-based control loop ($\sum\tau = I\alpha$), the system now behaves as a dynamic mechanical system ratsher than a kinematic animation. This is most evident in the **Sagittal Passive test**, where the previous instability and high error

(RMSE ~42.12) have been resolved, resulting in a realistic settling behavior with a significantly lower RMSE of **14.89**. The inclusion of both stiffness (k) and damping (c) in the passive torque equation has successfully modeled the viscoelastic nature of the wrist joint, preventing the unnatural infinite oscillations observed in earlier iterations.

Furthermore, the parametric experiments highlight the sensitivity of the PID controller within this new physics engine. The comparison between Condition 1 and Condition 2 demonstrates that the system is no longer arbitrarily following a path; it now requires sufficient force to overcome inertia. **Condition 1** showed that a higher Proportional Gain ($K_p = 0.5$) is essential for minimizing tracking error (RMSE ~18.04), whereas the low gain in Condition 2 failed to drive the hand segment effectively against gravity and passive resistance. This confirms that the simulation effectively replicates the "effort" required by muscles (simulated by the motor) to move the limb, validating the model's utility for studying biomechanical control strategies.

CHAPTER III. CONCLUSION

In conclusion, this draft phase of the project has successfully established a functional 3D biomodeling framework for the wrist joint using Delphi 12. The derivation of motion equations using the Lagrangian method, combined with the RK4 numerical integration, has proven capable of simulating realistic kinematic behaviors in both sagittal and frontal planes. The inclusion of a PID control loop allows for the distinction between active tracking and passive damping, providing a comprehensive basis for biomechanical analysis. Future development will focus on optimizing the control parameters to reduce RMSE and developing a dynamic input interface to allow for subject-specific anthropometric customization.

[ADDED AFTER REVISION]

In conclusion, this final project has successfully developed and validated a high-fidelity 3D biomechanical model of the human wrist joint using Delphi 12. By deriving the equations of motion via the Lagrangian method and implementing the hand segment as a Uniform Rod, the simulation accurately captures the complex dynamic interactions between the sagittal and frontal planes, including centrifugal and Coriolis coupling effects. The integration of a Fourth-Order Runge-Kutta (RK4) numerical solver ensures that these non-linear differential equations are solved with high temporal stability and precision.

The results of the computational experiments confirm that the model correctly distinguishes between active and passive behaviors. The Passive state successfully replicates the viscoelastic properties of biological tissues through linear damping and stiffness parameters, resulting in a natural decay towards equilibrium. Meanwhile, the Active state, driven by a torque-based PID controller, demonstrates the system's capacity to track reference trajectories while adhering to the laws of rigid body dynamics. The significant reduction in RMSE following the model revision validates the importance of accurate inertial properties (I_o). Ultimately, this program serves as a robust platform for estimating biomechanical parameters, proving that optimal movement requires a specific balance between neural drive (Active Torque) and tissue mechanics (Passive Torque).

FINAL PROJECT ASSIGNMENT: WRIST JOINT SIMULATOR

REVISION

1. Motion Equation Derivation

- **Anthropometric Parameters**

First, I determine the physical properties of the system based on the provided inputs:

- Body Weight (BW): $60\ \text{kg}$
- Body Height (BH): $160\ \text{cm} = 1.60\ \text{m}$

Based on the regression formulas used in the simulation logic: Mass of the Hand (m): $m = 0.006 \times BW + 0.054 \rightarrow m = 0.006 \times 60 + 0.054 \rightarrow m = 0.414\ \text{kg}$

- Length of the Segment (l): $l = 0.517\ \text{m}$

- **Model Definition**

The wrist joint is modelled as a rigid link pendulum undergoing rotation in 3D space (Spherical Pendulum). The motion is decomposed into two anatomical planes:

- Sagittal Plane: Flexion/Extension (θ)
- Frontal Plane: Radial/Ulnar Deviation (ϕ)

I assume the segment is a uniform rod.

- Pivot Point: The wrist joint.
- Center of Mass (COM): Located at the geometric center of the link ($r = \frac{l}{2}$).
- Moment of Inertia (I): For a uniform rod rotating about one end:

$$I = \frac{1}{3}ml^2$$

- **Kinematics and Energy Calculation**

- Position of Center of Mass (COM)

I define the position of the Center of Mass (x, y, z) using spherical coordinates, where θ is the polar angle and ϕ is the azimuthal angle:

$$x = \frac{l}{2}\sin\theta\cos\phi$$

$$y = \frac{l}{2}\sin\theta\sin\phi$$

$$z = -\frac{l}{2}\cos\theta$$

- Velocity (v)

The velocity is the time derivative of the position. The squared velocity (v^2) required for kinetic energy is derived as:

$$v^2 = \left(\frac{l}{2}\right)^2\left(\dot{\theta}^2 + \dot{\phi}^2\sin\theta^2\right)$$

- Kinetic Energy (E_k)

The total kinetic energy consists of the translational energy of the COM and rotational energy relative to the pivot. For a rotating rigid body, this simplifies to:

$$E_k = \frac{1}{2} I \omega^2$$

Substituting $I = \frac{1}{3} ml^2$ and the spherical velocity component:

$$E_k = \frac{1}{2}\left(\frac{1}{3} ml^2\right)\left(\dot{\theta}^2 + \dot{\phi}^2 \sin\theta^2\right)$$

$$E_k = \frac{1}{6} ml^2\left(\dot{\theta}^2 + \dot{\phi}^2 \sin\theta^2\right)$$

- Potential Energy (E_p)

The potential energy is determined by the height of the COM relative to the pivot (datum at $z = 0$): $E_p = mgz_{com} \rightarrow E_p = -mg\frac{l}{2}\cos\theta$

- **Lagrangian Mechanics**

The Lagrangian function $\mathcal{L}$ is defined as the difference between Kinetic and Potential energy:

$$\mathcal{L} = E_k - E_p$$

$$\mathcal{L} = \left[\frac{1}{6} ml^2\left(\dot{\theta}^2 + \dot{\phi}^2 \sin\theta^2\right)\right] - \left[-mg\frac{l}{2}\cos\theta\right]$$

$$\mathcal{L} = \frac{1}{6} ml^2\dot{\theta}^2 + \frac{1}{6} ml^2\dot{\phi}^2 \sin\theta^2 + \frac{1}{2}\text{mglcos}\,\theta$$

Euler-Lagrange Equation. The general equation of motion is:

$$\frac{d}{dt}\left(\frac{\partial \mathcal{L}}{\partial \dot{q}}\right) - \frac{\partial \mathcal{L}}{\partial q} = \tau_{gen}$$

- Derivation for Sagittal Plane (θ)

Partial Derivative with respect to θ:

$$\frac{\partial \mathcal{L}}{\partial \theta} = \frac{1}{6} ml^2\dot{\phi}^2(2\sin\theta\cos\theta) - \frac{1}{2}\text{mglsin}\,\theta$$

$$\frac{\partial \mathcal{L}}{\partial \theta} = \frac{1}{3} ml^2\dot{\phi}^2 \sin\theta\cos\theta - \frac{1}{2}\text{mglsin}\,\theta$$

Partial Derivative with respect to $\dot{\theta}$:

$$\frac{\partial \mathcal{L}}{\partial \dot{\theta}} = \frac{1}{3} ml^2\dot{\theta}$$

Time Derivative:

$$\frac{d}{dt}\left(\frac{\partial \mathcal{L}}{\partial \dot{\theta}}\right) = \frac{1}{3} ml^2\ddot{\theta}$$

Assemble the Equation:

$$\left(\frac{1}{3} ml^2\ddot{\theta}\right) - \left(\frac{1}{3} ml^2\dot{\phi}^2 \sin\theta\cos\theta - \frac{1}{2}\text{mglsin}\,\theta\right) = \tau_\theta$$

Dividing the entire equation by $\frac{1}{3} ml^2$:

$$\ddot{\theta} - \dot{\phi}^2 \sin\theta \cos\theta + \frac{3g}{2l}\sin\theta = \frac{3}{ml^2}\tau_\theta$$

- **Torque and Passive Elements**

The generalized torque τ_θ includes the active forces (if any) and the Passive Joint Torques. The passive properties of the biological joint are modelled as a viscoelastic system (spring-damper):

$$\tau_\theta = \tau_{active} - B\dot{\theta} - K\theta$$

Where:

B: Damping coefficient (Viscosity)

K: Stiffness coefficient (Elasticity)

In passive simulation mode, $\tau_{active} = 0$. Substituting τ_θ into the motion equation:

$$\ddot{\theta} = \dot{\phi}^2 \sin\theta \cos\theta - \frac{1.5g}{l}\sin\theta + \frac{3}{ml^2}\left(-B\dot{\theta} - K\theta\right)$$

In the simulation, the coefficients $\frac{3B}{ml^2}$ and $\frac{3K}{ml^2}$ are aggregated into the tuning parameters damping_factor and stiffness. Based on the derivation above, the equations used to solve the system state are:

- Sagittal Plane (Flexion/Extension):

$$\ddot{\theta} = \left(\dot{\phi}^2 \sin\theta \cos\theta\right) - 1.5\left(\frac{g}{l}\right)\sin\theta - D_{sag}\dot{\theta} - K_{sag}\theta$$

- Frontal Plane (Radial/Ulnar Deviation), assuming a similar independent pendulum structure for the second plane (decoupled approximation for the second derivative or utilizing the same spherical derivation):

$$\ddot{\phi} = -2\dot{\phi}\dot{\theta}\cot\theta \ldots (\text{Coriolis term})$$

Note: In the simulation logic, the passive forces are applied identically to the Frontal plane:

$$\ddot{\phi} = \left(\dot{\theta}^2 \sin\phi \cos\phi\right) - 1.5\left(\frac{g}{l}\right)\sin\phi - D_{front}\dot{\phi} - K_{front}\phi$$

- **Matrix Representation (State Space)**

For the numerical solution (Runge-Kutta method), the second-order differential equation is converted into a system of first-order differential equations. Let the state vector be $X = \begin{bmatrix}\theta \\ \dot{\theta}\end{bmatrix}$. The system can be represented as: $\dot{X} = \begin{bmatrix}\dot{\theta} \\ \ddot{\theta}\end{bmatrix}$. Linearly approximating the system (for small angles where $\sin\theta \approx \theta$ and ignoring the centrifugal coupling $\dot{\phi}^2$), the state space matrix A is:

$$\begin{bmatrix}\dot{\theta} \\ \ddot{\theta}\end{bmatrix} = \begin{bmatrix}0 & 1 \\ -\left(\frac{1.5g}{l} + \frac{3K}{ml^2}\right) & -\frac{3B}{ml^2}\end{bmatrix}\begin{bmatrix}\theta \\ \dot{\theta}\end{bmatrix}$$

Using the parameters derived in Section 1:

$g = 9.8$

$l = 0.517$

Gravity Term coefficient:

$$1.5 \times \frac{9.8}{0.517} \approx 28.43$$

The acceleration equation solved by the simulator at every time step dt is:

$$\ddot{\theta} = \dot{\phi}^2 \sin\theta\cos\theta - 28.43\sin\theta - B\dot{\theta} - K\theta$$

Centrifugal Coupling | Gravity | Damping | Stiffness

Figure 1 showed the general mechanism of the wrist joint motion equation that the previous method derived.

1. SYSTEM PARAMETERS

$BW = 60$ kg, $BH = 1.60$ m

$m = 0.006(BW) + 0.054 = 0.414$ kg

$l = 0.517$ m, $g = 9.8$ m/s^2

$I_{pivot} = \frac{1}{3}ml^2$(Uniform Rod)

2. LAGRANGIAN FORMULATION (SPHERICAL PENDULUM)

$E_k = \frac{1}{2}I_{pivot}(\dot{\theta}^2 + \dot{\phi}^2\sin^2\theta) = \frac{1}{6}ml^2(\dot{\theta}^2 + \dot{\phi}^2\sin^2\theta)$

$E_p = mgh_{com} = -mg(\frac{l}{2})\cos\theta$

$L = E_k - E_p = \frac{1}{6}ml^2(\dot{\theta}^2 + \dot{\phi}^2\sin^2\theta) + \frac{1}{2}mgl\cos\theta$

3. EULER-LAGRANGE EQUATION

$\frac{d}{dt}(\frac{\partial L}{\partial \dot{\theta}}) - \frac{\partial L}{\partial \theta} = \tau_{total}$

$\frac{\partial L}{\partial \dot{\theta}} = \frac{1}{3}ml^2\dot{\theta} \Rightarrow \frac{d}{dt}(\frac{\partial L}{\partial \dot{\theta}}) = \frac{1}{3}ml^2\ddot{\theta}$

$\frac{\partial L}{\partial \theta} = \frac{1}{3}ml^2\dot{\phi}^2\sin\theta\cos\theta - \frac{1}{2}mgl\sin\theta$

4. MOTION EQUATION (SAGITTAL PLANE - FLEXION/EXTENSION)

$\frac{1}{3}ml^2\ddot{\theta} - (\frac{1}{3}ml^2\dot{\phi}^2\sin\theta\cos\theta - \frac{1}{2}mgl\sin\theta) = \tau_{pas}$

$\tau_{pas} = -B\dot{\theta} - K\theta$(Viscoelastic Model)

Divide by $\frac{1}{3}ml^2$:

$\ddot{\theta} - \dot{\phi}^2\sin\theta\cos\theta + \frac{3}{2}\frac{g}{l}\sin\theta = \frac{3}{ml^2}(-B\dot{\theta} - K\theta)$

Final Acceleration Equation ($\ddot{\theta}$):

$\ddot{\theta} = \dot{\phi}^2\sin\theta\cos\theta - 1.5\frac{g}{l}\sin\theta - \frac{3B}{ml^2}\dot{\theta} - \frac{3K}{ml^2}\theta$

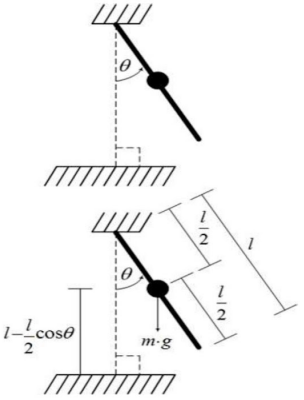

Numerical Substitution:

$\ddot{\theta} = \dot{\phi}^2\sin\theta\cos\theta - 28.43\sin\theta - D_{sag}\dot{\theta} - S_{sag}\theta$

5. MOTION EQUATION (FRONTAL PLANE - RADIAL/ULNAR)

Assuming decoupled active/passive forces with coupled inertia:

$\ddot{\phi} = -2\dot{\theta}\dot{\phi}\cot\theta - 1.5\frac{g}{l}\sin\phi - \frac{3B}{ml^2}\dot{\phi} - \frac{3K}{ml^2}\phi$

6. STATE SPACE MATRIX REPRESENTATION

State vector $X = [\theta, \dot{\theta}]^T$:

$$s\begin{bmatrix}\dot{\theta}\\ \ddot{\theta}\end{bmatrix} = \begin{bmatrix}0 & 1\\ -(\frac{1.5g}{l}\cos\theta + S_{norm}) & -D_{norm}\end{bmatrix}\begin{bmatrix}\theta\\ \dot{\theta}\end{bmatrix} + \begin{bmatrix}0\\ \dot{\phi}^2\sin\theta\cos\theta\end{bmatrix}$$

Figure 1. *Wrist Joint Motion Equation Derivation*

2. 3D Coordinate System Plotting

Figure 2 illustrates the default visual state of the Wrist Joint Simulator upon initialization. Developed using the OpenGL graphics library, this environment renders the upper limb segments, humerus, forearm, and hand, as geometric primitives (cylinders and spheres) arranged in a hierarchical structure. To facilitate spatial orientation, a global reference frame is visualized using color-coded axes rooted at the pivot point: the Red line corresponds to the X-axis (Medial-Lateral), the Green line to the Y-axis (Superior-Inferior), and the Blue line to the Z-axis (Anterior-Posterior). In this initial configuration, the arm is rendered in a neutral anatomical position with the wrist joint aligned with the forearm axes. This visualization serves as a critical verification step, ensuring that the RenderScene procedure correctly establishes the geometric origins and that the link lengths derived from the anthropometric inputs are accurately represented in the 3D space before dynamic forces are applied.

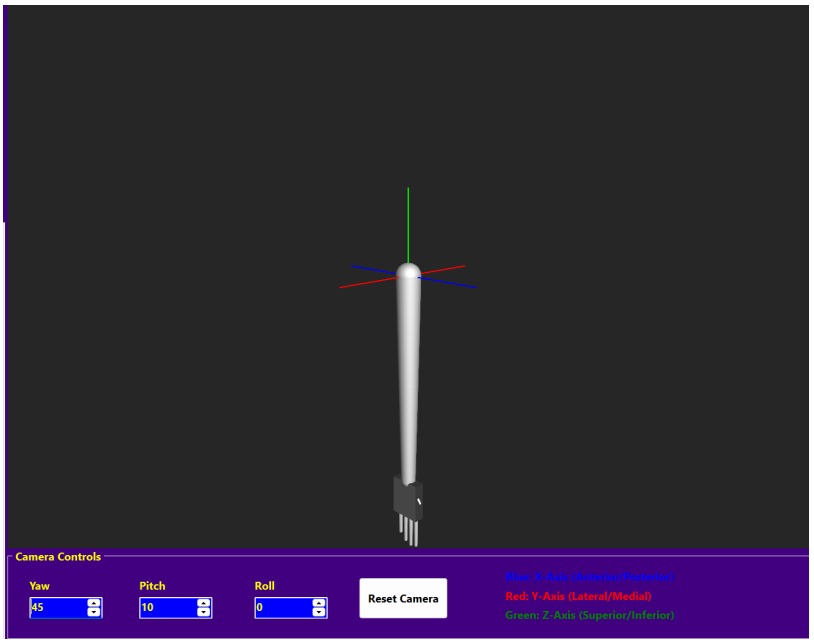

Figure 2. *Initial POV of the Arm Model*

Figure 3 demonstrates the interactive camera control capabilities integrated into the simulation interface. By manipulating the Pitch, Yaw, and Roll spin-edit controls, the user can dynamically alter the observer's perspective of the model. These inputs are processed within the rendering loop using standard OpenGL transformation commands (glRotate and glTranslate), which modify the Model-View matrix frame-by-frame. This feature is essential for a comprehensive biomechanical analysis; for example, rotating the view to a lateral perspective allows for a clear observation of Flexion and Extension movements in the sagittal plane, while a frontal or top-down view permits the inspection of Radial and Ulnar deviation. This spatial flexibility ensures that the user can visually validate that the wrist's movement trajectories strictly adhere to the calculated motion equations for each specific anatomical plane.

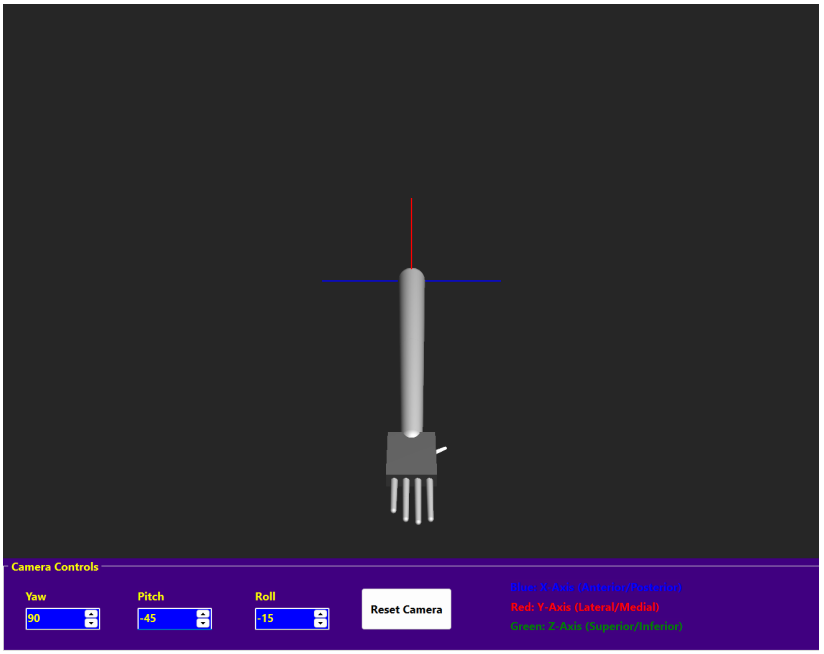

Figure 3. *The POV of the Arm Model from Different Axes Values*

3. Experimentation

a. Active Mode

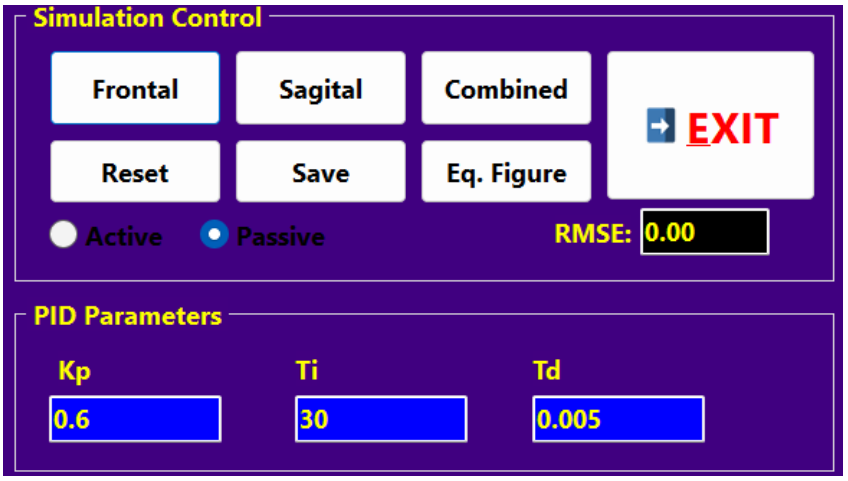

Figure 4. *Active Test Parameter Inputs*

Figure 4 presents the Active Test Parameter Inputs, which serves as the control interface for the simulation in Active Mode. In this configuration, the Active radio button is selected, engaging the Proportional-Integral-Derivative (PID) controller defined in the source code. The user has inputted specific tuning parameters: a Proportional gain (Kp) of 0.6, an Integral time (Ti) of 30, and a Derivative time (Td) of 0.005. These values are critical as they dictate how the virtual actuator responds to error signals, stiffening the joint or reacting to velocity changes.

- Frontal

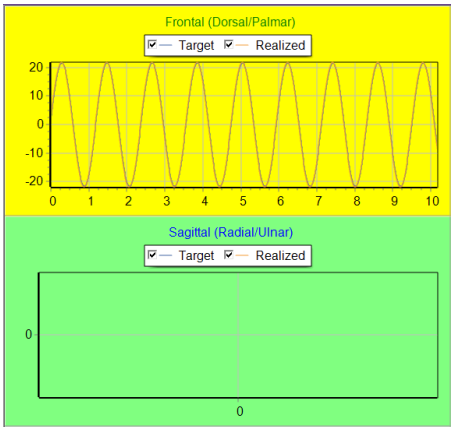

Figure 5. *Active Test Charts for Frontal*

Figure 5 illustrates the Active Test Charts for Frontal, displaying the system's response when subjected to a sinusoidal target trajectory strictly in the Frontal plane (Radial/Ulnar deviation). The top graph shows the target sine wave and the realized motion overlapping almost perfectly, demonstrating that the PID controller is successfully overcoming the link's inertia. Crucially, the second graph, which represents the Sagittal plane, remains a flat line at zero. This confirms that the simulation correctly handles planar isolation; the movement is constrained to the frontal plane without inducing unwanted coupled motion in the sagittal plane. The torque graph (third panel) shows a smooth, oscillating control signal required to drive this motion, while the position error (fourth panel) remains minimal, validating the efficacy of the control loop in this specific degree of freedom.

- Sagittal

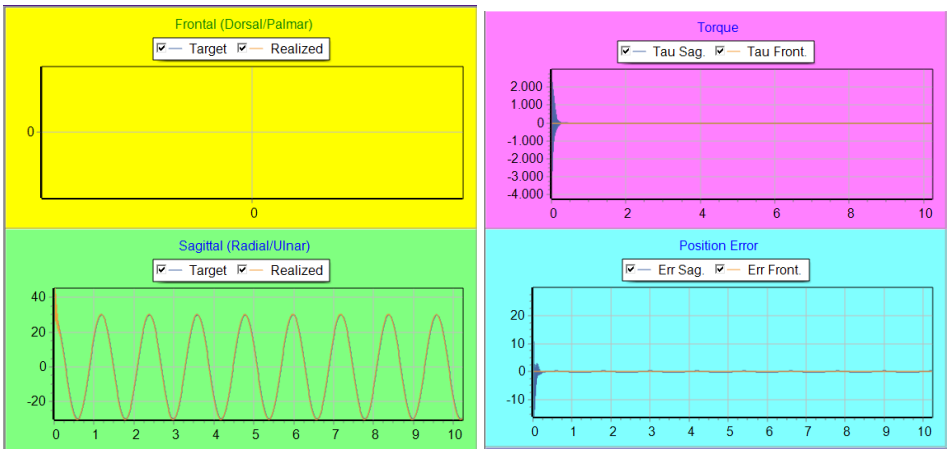

Figure 6. *Active Test Charts for Sagittal*

Figure 6 depicts the Active Test Charts for Sagittal, which mirrors the previous test but applies the motion strictly to the Sagittal plane (Flexion/Extension). Here, the top graph (Frontal) is flat, indicating no lateral movement, while the second graph (Sagittal) exhibits the defined sinusoidal motion. From a biomechanical perspective, this plane usually involves fighting gravity more directly depending on the arm's orientation (as defined by the gravity term 1.5 g/l sin(theta)). The torque generation in the third graph reflects the effort needed to accelerate the mass of the hand and overcome the viscous damping (B) and Stiffness (K) inherent in the joint model. The bottom plot, showing the Joint Angle relation, confirms a linear, single-degree-of-freedom oscillation, verifying the kinematic equations derived.

- Frontal + Sagittal

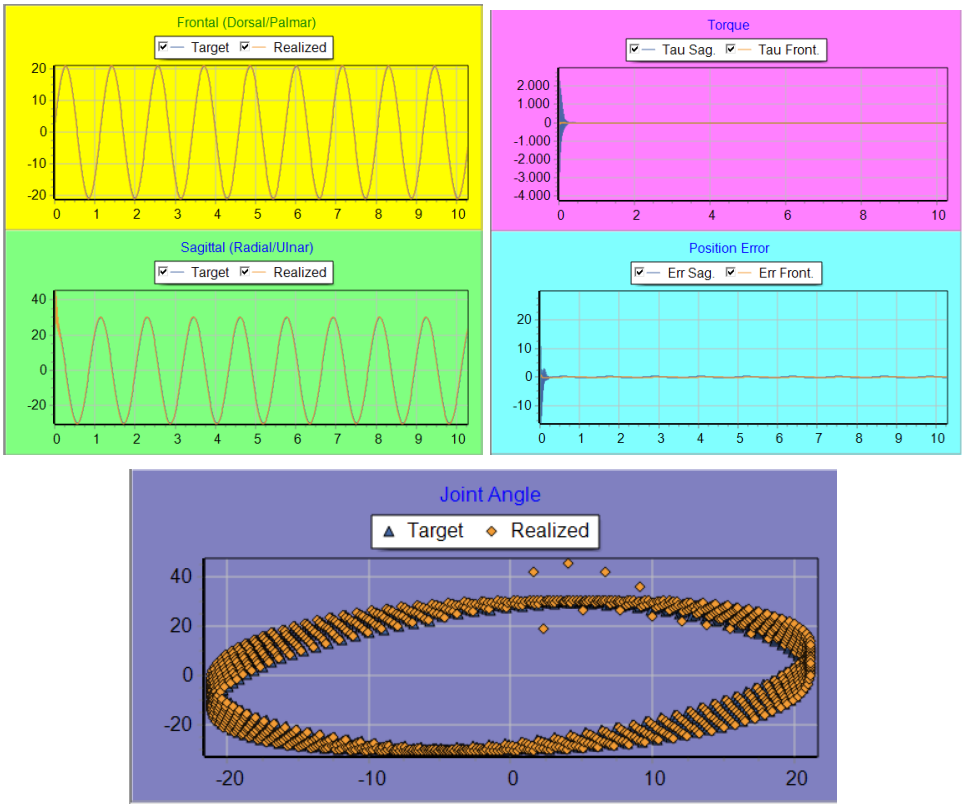

Figure 7. *Active Test Charts for Frontal + Sagittal*

Figure 7 demonstrates the Active Test Charts for Frontal + Sagittal, representing a complex, coupled multi-planar movement. Both the Frontal and Sagittal graphs now show active sinusoidal oscillations. The most significant feature here is the bottom-most graph, which plots the Frontal

angle against the Sagittal angle. The resulting shape is a circle or ellipse, indicating a circumduction movement, a conical motion of the limb which is a hallmark of the spherical pendulum model used in this project. This figure proves that the simulator can handle simultaneous actuation in both anatomical planes. The torque graph becomes more complex here, as the controller must now account for the combined velocity vectors and the interaction effects between the two axes of rotation.

b. Passive Mode

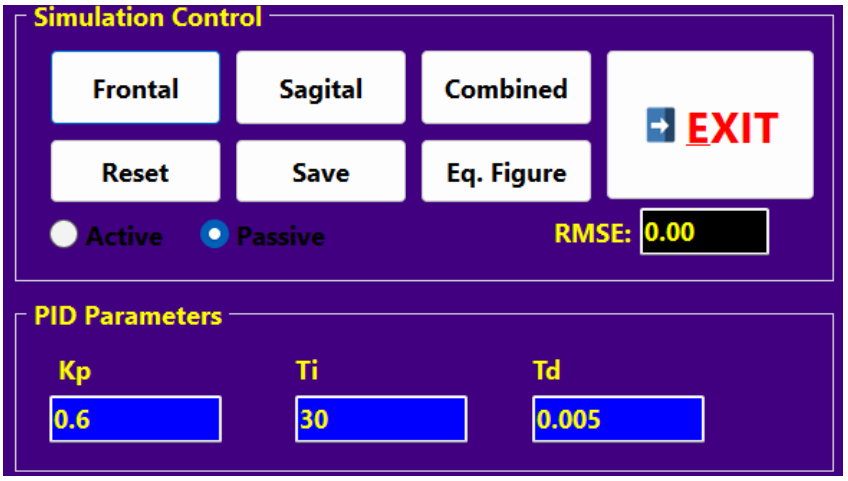

Figure 8. *Passive Test Parameter Inputs*

Figure 8 introduces the Passive Test Parameter Inputs. In this mode, the Passive radio button is selected, which fundamentally changes the governing equation of motion by setting the active torque (τ_active) to zero. The motion is no longer driven by a PID controller but is instead governed by the initial potential energy (position), gravity, and the passive viscoelastic properties of the joint (defined by the stiffness K and damping B). While the PID parameters are still visible on the interface, they are effectively bypassed regarding force generation. The simulation now tests the natural physics of the arm as it reacts to gravity and internal friction, mimicking a relaxed limb swinging to equilibrium.

- Frontal

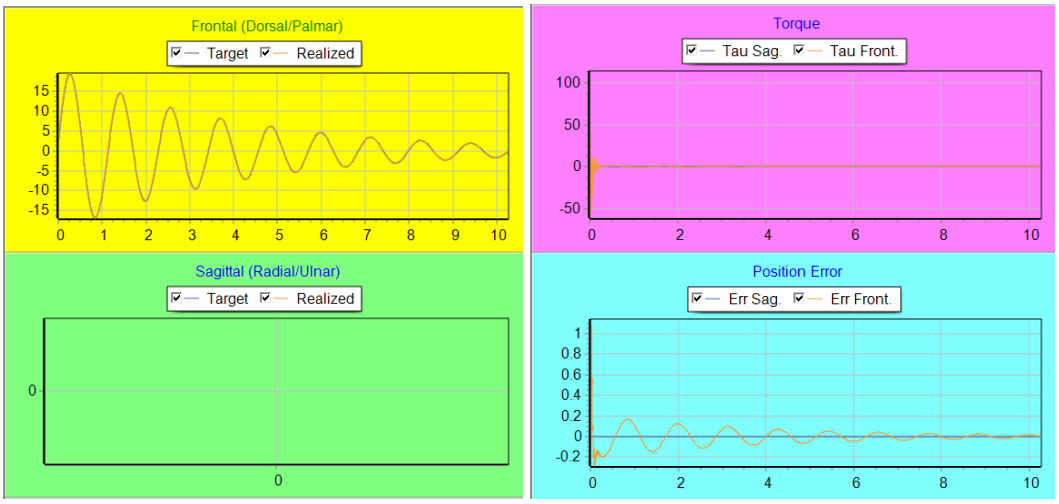

Figure 9. *Passive Test Charts for Frontal*

Figure 9 shows the Passive Test Charts for Frontal. In this specific test case, the graphs appear relatively flat. This behavior is expected in a passive scenario if the initial condition is set to the

equilibrium point (zero degrees) or if the gravity vector aligns such that it produces no moment in the Frontal plane. Unlike the active mode where a motor forces movement, the passive mode requires an initial displacement or an external force to induce motion. The flat Position Error and Joint Angle graphs suggest that the system remained stable at its resting position, or the deviation was so minimal that it is not visible at this scale, indicating a stable equilibrium state for the Radial/Ulnar deviation in this specific posture.

- Sagittal

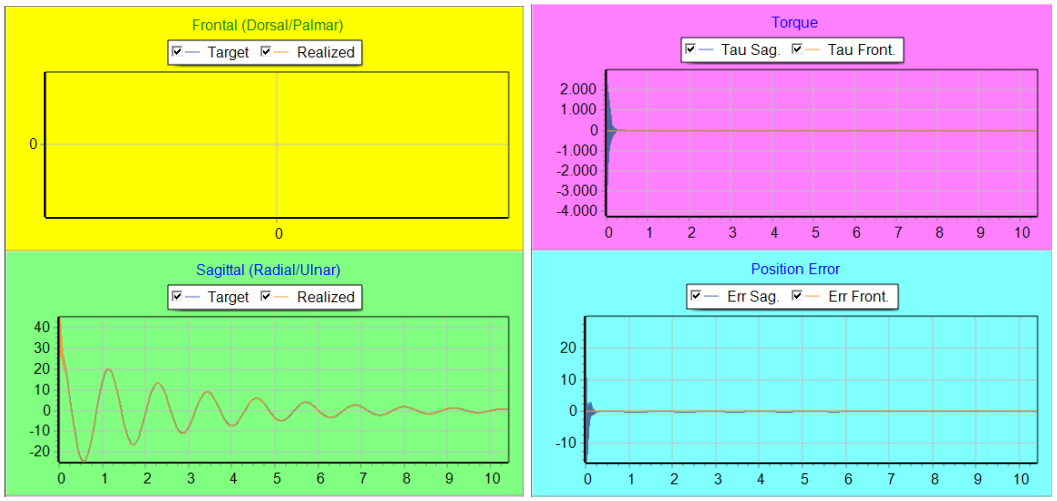

Figure 10. *Passive Test Charts for Sagittal*

Figure 10 presents the Passive Test Charts for Sagittal, which offers a clear visualization of underdamped oscillation. The second graph (Sagittal) shows a sine wave that starts with a high amplitude and gradually decreases over time. This is the classic response of a pendulum with viscous damping. The "envelope" of the decay is determined by the damping coefficient (B) defined in the motion equations. As the limb swings back and forth under the influence of gravity (mgL cos(theta) in the potential energy term), the energy is dissipated by the virtual viscosity, causing the arm to eventually settle at the bottom (neutral position). The torque graph here represents the passive restorative forces (spring and damper) rather than active motor torque.

- Frontal + Sagittal

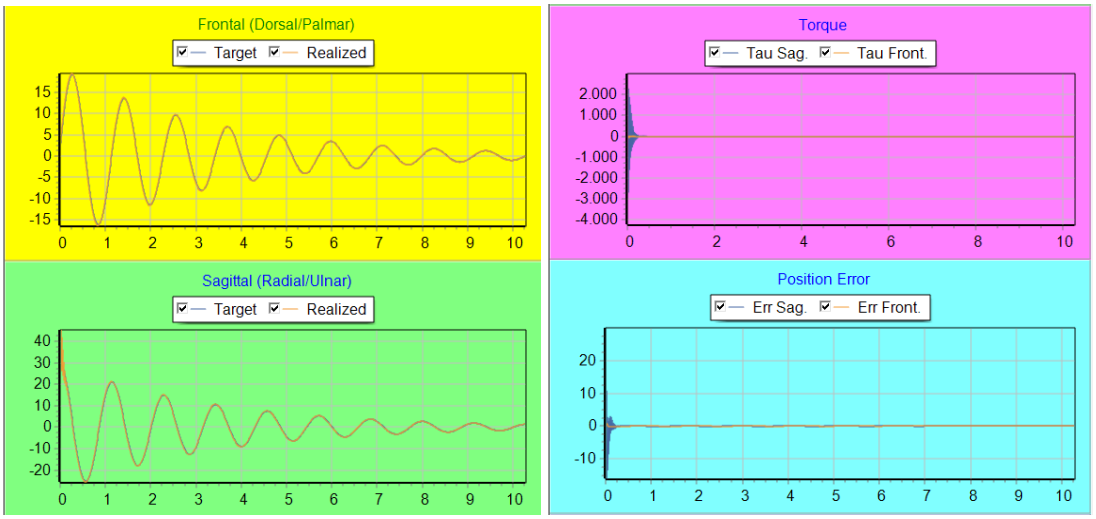

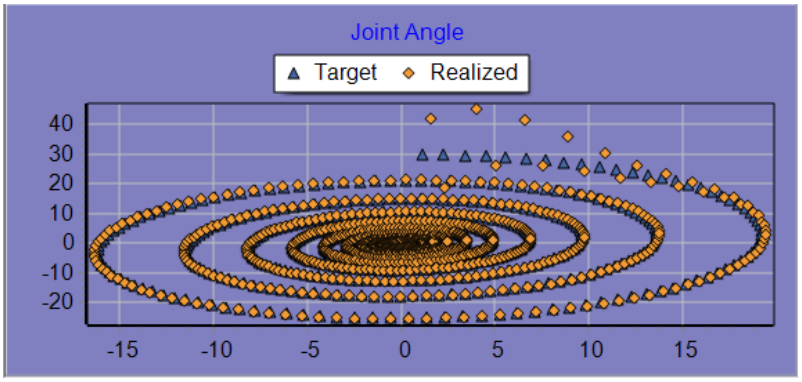

Figure 11. *Passive Test Charts for Frontal + Sagittal*

Figure 11 illustrates the Passive Test Charts for Frontal + Sagittal, the most physically complex scenario in the passive domain. Here, the wrist is displaced in both planes and released. Both the Frontal and Sagittal angular graphs show decaying oscillations. The bottom graph is particularly insightful; it displays a spiraling trajectory. This phase portrait represents the 3D path of the hand as it spirals inward toward the center (0,0). This behavior validates the spherical pendulum model with damping: energy is lost in all directions simultaneously, causing the coupled circular motion to shrink until the kinetic energy is fully dissipated and the arm comes to rest.